European Journal of Pharmaceutics and Biopharmaceutics 145 (2019) 12–26

Contents lists available at ScienceDirect

European Journal of Pharmaceutics and Biopharmaceutics

journal homepage: www.elsevier.com/locate/ejpb

Hybrid nanocrystal–amorphous solid dispersions (HyNASDs) as alternative to ASDs for enhanced release of BCS Class II drugs

Mahbubur Rahman, Faustin Arevalo, Alexander Coelho, Ecevit Bilgili*

Otto H. York Department of Chemical and Materials Engineering, New Jersey Institute of Technology, University Heights, Newark, NJ 07012, USA

ARTICLE INFO

Keywords:
Wet stirred media milling
Spray drying
Nanoparticles
Nanocomposites
Amorphous solid dispersion
Dissolution

ABSTRACT

A major shortcoming of drug nanocomposites as compared with amorphous solid dispersions (ASDs) is their limited supersaturation capability in dissolution media. Here, we prepared drug hybrid nanocrystal–amorphous solid dispersions (HyNASDs) and compare their performance to ASDs. A wet-milled griseofulvin (GF, BCS II drug) nanosuspension and a GF solution, both containing the same dissolved polymer–surfactant (SDS: sodium dodecyl sulfate) with 1:1 and 1:3 GF:polymer mass ratios, were spray-dried. Hydroxypropyl cellulose (HPC) and Soluplus (Sol) were used as matrix-forming polymers. XRPD, DSC, and Raman spectroscopy reveal that ASDs were formed upon spray-drying the solution-based feed, whereas nanocomposites and nanocomposites with > 10% amorphous content, HyNASDs, were formed with the nanosuspension-based feed. Sol provided higher GF relative supersaturation, up to 180% and 360% for HyNASDs and ASDs, respectively, in the dissolution tests than HPC (up to 50% for both) owing to Sol's stronger intermolecular interactions and miscibility with GF and its recrystallization inhibition. Besides the higher kinetic solubility of GF in Sol, presence of GF nanoparticles vs. micron-sized particles in the nanocomposites enabled fast supersaturation. This study demonstrates successful preparation of fast supersaturating (190% within 20 min) HyNASDs, which renders nanoparticle formulations competitive to ASDs in bioavailability enhancement of poorly soluble drugs.

1. Introduction

It is estimated that about 40% of the marketed drugs and 90% of the drug molecules in the development pipeline are characterized as poorly water-soluble [1]. As these drugs dissolve slowly, their intestinal absorption turns out to be rate-limiting, leading to low bioavailability [2,3]. Significant academic and industrial research has been directed toward developing various formulation/processing approaches for the dissolution enhancement of poorly water-soluble drugs [4–12]. Among all these approaches, two formulation approaches have been widely used in the pharmaceutics literature and marketed products: nanocrystal-based solid dosage forms (nanocomposites) and amorphous solid dispersions (ASDs) [12–16]. In a nanocomposite, drug is usually dispersed in a polymeric matrix as a secondary phase in the form of nanocrystals [16,17], whereas in an ASD, it is molecularly dispersed in the matrix of a miscible, amorphous polymer [15].

Nanocrystals have larger specific surface area than typical micron-sized drug crystals, and they can therefore enhance the dissolution rate of BCS Class II drugs [18–20] according to the Noyes–Whitney equation [21], and, in turn, their bioavailability. Moreover, nanocrystals especially those with sizes less than ~100 nm have very high curvature and tend to show increased saturation solubility, which also enhances the dissolution rate, and this phenomenon can be explained via the Kelvin and the Ostwald–Freundlich equation [22]. The higher apparent solubility that originates from the greater curvature of 100 nm nanocrystals than that of the micron-sized crystals was estimated to be ~10–15%, typically for a drug candidate with a molecular weight of 500 g/mol, density of 1 kg/m^3, and a crystal medium interfacial tension of 0.015–0.020 N/m [23]. On the other hand, Muller and Peters [24] observed up to 50% increase in the apparent solubility of an insoluble antimicrobial compound when particle size was reduced from 2.4 μm to 300 nm. Fu et al. [25] produced nimodipine nanosuspensions with mean diameters down to 160 nm. In dissolution tests, the lyophilized nimodipine suspensions with maltose and mannitol exhibited no supersaturation, < 50% supersaturation, and ~100% supersaturation in FaSSIF, 0.05% SDS solution, and purified water as the dissolution media, respectively. Hence, it is fair to assert that nanocrystal formulations have not been widely tested under supersaturating conditions in dissolution tests unlike the case for ASDs (see e.g. [26,27]).

Drug nanosuspensions are most commonly produced by wet stirred

* Corresponding author at: Otto H. York Department of Chemical and Materials Engineering, New Jersey Institute of Technology, 161 Warren St. 150 Tiernan Hall, Newark, NJ 07102, USA.
E-mail address: bilgece@njit.edu (E. Bilgili).

https://doi.org/10.1016/j.ejpb.2019.10.002
Received 3 July 2019; Received in revised form 9 October 2019; Accepted 11 October 2019
Available online 14 October 2019
0939-6411/

Table 1
Formulations and drug–polymer content of nanosuspensions used for the preparation of spray-dried nanocomposites in recent studies.

Drug	Drug content (% w/v)	Polymeric stabilizer[b]	Drug:polymer mass ratio	References
Naproxen	1.0	HPMC	1:0.5	Kumar et al. [36]
Lovastatin	0.5[a]	PVP K12, K30, K17, and PVA	1:0.2	Zhang et al. [37]
Griseofulvin	10[a]	HPC SL	1:0.25	Azad et al. [27]
Naproxen	1.0, 3.0, and 5.0	HPMC E15	1:0.2–1:0.6	Kumar et al. [38]
Griseofulvin	5.0	HPC SL	1:0.25	Shah et al. [39]
Allisartan Isoproxil	5.0	PVP K30	1:0.01–1:0.03	Hou et al. [40]
Mefenamic Acid	5.0[a]	HPC SSL	1:0.15	Konnerth et al. [41]
Aprepitant	2.5	Pharmacoat 603 and HPC SSL	1:0.5, 1:1	Toziopoulou et al. [42]
Carvedilol	8.3	HPC SL	1:0.1–1:0.4	Medarevic et al. [43]
Fenofibrate	10.0[a]	HPC	1:0.25	Aleandri et al. [44]
Itraconazole	10.0[a]	HPC SL	1:0.25–1:0.65	Li et al. [45]
Itraconazole	10.0[a]	HPC L and HPC SL	1:0.45	Bilgili et al. [46]

[a] With respect to the total weight of the suspension liquid (% w/w); [b]HPMC: hydroxypropyl methylcellulose, HPC: hydroxypropyl cellulose, PVA: polyvinyl alcohol, PVP: polyvinylpyrrolidone.

media milling (WSMM) [16]. The aggregation–growth tendency of drug nanocrystals during milling or storage poses serious challenges [28]. Usually, hydrophilic/amphiphilic polymers and/or surfactants are added to the suspensions as stabilizers to suppress the aggregation [28,29]. In general, drug:stabilizer mass ratio has been optimized based on several considerations. At low concentration of stabilizers, drug nanoparticle aggregation cannot be suppressed [30,31]; while if used in excess, stabilizers especially surfactants may promote Ostwald ripening [32,33]. Finally, stabilizer concentration should be minimized to achieve high drug loading in the final solid dosages, while still achieving physical stability in the milled suspensions [16,28]. In view of these considerations, it is no surprise to find that a drug:polymer mass ratio much higher than 1 has been widely reported: 1:0.5–1:0.05 [13,29], 1:0.8–1:0.02 [34], and 1:1–1:0.02 [35]. A quick review of recent literature (see refs. [27,36–46] in Table 1) also suggests a similarly high drug:polymer mass ratio, i.e., 1:1 to 1:0.01, in drug nanosuspensions used in the preparation of spray-dried nanocomposites.

Due to the convenience of usage and patient compliance, nanosuspensions are usually dried into nanocomposite microparticles or shortly nanocomposites, which are ultimately incorporated into standard dosage forms such as tablet, capsule, and sachets [26,47,48]. Drying of drug nanosuspensions has been carried out by various processes [16]; among them, spray-drying [27,49] is one of the most cost-effective continuous process [16,50]. Nanocomposites prepared via spray drying increased drug dissolution rate and enhanced the bioavailability (see e.g. [40]). The most serious limitation of drug nanocomposites is their limited supersaturation generation capability during dissolution. Interestingly, even though all studies mentioned in Table 1 reported significant increase in drug release from the spray-dried nanocomposites as compared with as-received drug micro-crystals and their physical mixtures with the excipients, none of these studies investigated or reported any supersaturation generation in the dissolution tests.

Another platform formulation approach for bioavailability enhancement of the poorly water-soluble drugs is drug ASD, wherein drug molecules are molecularly dispersed into or solubilized by an amorphous polymer. Since the apparent solubility of the amorphous form is much greater than its crystalline counterpart, ASDs provide higher extent of drug release and supersaturation [51–53]. Spray-drying has emerged to be the most popular solvent-based process to produce ASDs [54], while hot melt extrusion (HME) has become the standard fusion-based process to produced ASDs [55].

Surprisingly, although both drug nanocomposites and ASDs have been used as two major platforms for dissolution enhancement, a *head-to-head* comparison of *in vitro* drug release from these two solid dosage forms having *identical formulation* is not available in the literature. In some cases, nanosuspensions, not dried nanocomposites, were compared with ASDs, but not in a head-to-head manner. For instance, Fakes et al. [56] investigated the bioavailability enhancement of a BCS Class II drug, BMS-488043, using a 10% (w/w) drug nanosuspension with 2% (w/w) hydroxypropyl cellulose (HPC-SL) and 0.1% (w/w) sodium lauryl sulfate (SLS). They also prepared the drug ASD by spray drying and flash evaporation techniques at different drug:polymer (polyvinyl pyrrolidone, PVP) ratio. In the case of spray drying, 40:60 drug:PVP was used for the formulation development and further characterization, whereas 90:10 drug:PVP ratio was selected in the case of flash evaporation. The nanosuspension and two amorphous formulations containing 20% and 40% drug were compared to a wet-milled crystalline drug in a capsule in a crossover beagle dog study. While having different formulations, the ASDs showed superior bioavailability enhancement compared with the nanosuspension, as expected owing to relatively high drug supersaturation capability of the ASDs with respect to the nanosuspension. In a recent study [17], a nanoextrusion process was used to compare griseofulvin (GF) nanocomposites with ASDs. GF nanosuspensions prepared via WSMM were extruded with additional polymers and simultaneously dried in a twin-screw extruder. This nanoextrusion process with two different polymers, i.e., HPC (immiscible with GF) and Soluplus (Sol, miscible with GF), led to the formation of GF nanocomposite and GF ASD, respectively. The researchers demonstrated that for 100 mg GF dose, GF–Sol ASD led to 340% (relative) supersaturation whereas GF–HPC nanocomposite only achieved 60% supersaturation. While this finding corroborates the well-known shortcoming of nanocomposites vs. ASDs in drug supersaturation generation, a direct and scientifically fair *head-to-head* comparison of drug release from nanocomposites vs. ASDs having *identical polymer/formulation* is still lacking in the literature. Finally, none of the previous studies on spray-dried GF nanocomposites [26,27,39] reported or investigated GF supersaturation in the dissolution medium.

The main objective of this study is to enhance the limited supersaturation capability of drug nanocomposites in dissolution tests significantly by using a relatively low drug:polymer mass ratio (high polymer loading), i.e., 1:1 and 1:3, as compared with high drug:polymer mass ratio like 3:1 typical of nanocomposite formulations (Table 1). Ultimately, the special class of drug nanocomposites so produced, named here “Hybrid Nanocrystal–Amorphous Solid Dispersions” (HyNASDs), could be alternative to ASDs if HyNASDs are proven to provide drug supersaturation levels typical of ASDs. To this end, a wet media milled GF suspension and a GF solution, containing the same dissolved HPC/Sol–surfactant (SDS: sodium dodecyl sulfate) in water and acetone–water mixture were spray-dried to prepare GF nanocomposites/HyNASDs and GF ASDs, respectively. The particle size of the nanosuspensions and spray-dried powders was characterized via laser diffraction. The solid state of GF in the spray-dried powders was characterized by X-ray powder diffraction (XRPD) and differential scanning calorimetry (DSC), while GF–polymer molecular interactions were characterized by Raman spectroscopy. To elucidate the roles of drying rate and drug–polymer miscibility on recrystallization during

drying, a droplet of GF–polymer–SDS solution was dried on a heated microscope slide in quiescent air and visualized via polarized light microscope (PLM). GF recrystallization inhibition by HPC/Sol was examined via separate desupersaturation experiments. Redispersion experiments were performed to confirm recovery of drug nanoparticles from the nanocomposites/HyNASDs. Drug release from the spray-dried powders was investigated using USP II apparatus with UV-spectroscopy. To gain further insight, a loose compact of ASD particles with 1:3 GF:polymer was imbibed with water and GF recrystallization was visualized by PLM.

2. Materials and methods

2.1. Materials

BP/EP grade micronized griseofulvin (GF) was purchased from Letco Medical (Decatur, AL, USA) and used as a challenging Biopharmaceutics Classification System (BCS) Class II drug because GF nanocrystals exhibit severe aggregation in suspensions, if improperly stabilized [31], and it is known to be a fast crystallizing drug [57]. Clinical dose amount and Caco-2 permeability of GF are 125–500 mg/day and 130.94×10^{-6} cm/s, respectively [58,59]. Its solubility in deionized (DI) water is ~8.9 mg/L at 25 °C and ~14.2 mg/L at 37 °C; it has a melting point T_m of 220 °C and a glass transition temperature T_g of 89 °C [60]. Hydroxypropyl cellulose (HPC, SSL grade, Nisso America Inc., New York, NY) is a semi-crystalline polymer with low crystallinity and amorphous domains of very low T_g. It is widely used as a stabilizer during milling and matrix former in the nanocomposites [26,27]. Soluplus (Sol, BASF, Tarrytown, NY) is an amphiphilic graft copolymer produced from polyvinyl caprolactam–polyvinyl acetate–polyethylene glycol having a single glass transition temperature of 73 ± 2 °C [61]. Sol has been commonly used to produce ASDs of various poorly water-soluble drugs [62]. An anionic surfactant, sodium dodecyl sulfate (SDS), purchased from GFS Chemicals, Inc. (Columbus, OH) was used as a wetting agent, which also helps to stabilize GF nanosuspensions. Acetone (ACS reagent, ≥ 99.5%) was purchased from BDH Analytical chemicals, (VWR, GA) and used as a solvent to prepare solution-based feed to the spray dryer. In WSMM, Yttrium zirconia beads (Zirmil Y, Saint Gobain ZirPro, Mountainside, NJ, USA) with a median size of 430 μm were used.

2.2. Preparation of spray-dried powders

Aqueous suspension-based (W:water) feeds and organic solution-based (S:solvent) feeds of GF were fed to the spray dryer for the preparation of drug nanocomposites and ASDs, respectively (Fig. 1). Table 2 presents the formulations used in the precursor feeds. Drug concentration was kept constant at 2.5% (w/v). The GF concentration was calculated w.r.t. the total volume of the water in the suspension-based feeds and the total volume of the solvent mixture (acetone–-water) in the solution-based feeds, which was fixed at 240 mL. GF nanosuspensions were prepared with two different polymers (HPC/Sol) at 1:1 and 1:3 drug:polymer mass ratios to examine the impact of polymer type and polymer loading on GF release in dissolution tests. To elucidate the role of Sol, a nanosuspension with 3:1 GF:Sol (W-Sol-3:1) and a suspension of as-received (micronized) GF with 1:3 GF:Sol (W-M-Sol-1:3) were also prepared. In all formulations, SDS concentration was kept constant below the critical micelle concentration (CMC, 0.23%, w/v) at 0.125% (w/v) to minimize Ostwald ripening [30].

In the preparation of nanosuspension-based (W) feeds, a shear mixer (Fisher Scientific Laboratory Stirrer, Catalog No. 14-503, Pittsburgh, PA) was used to disperse as-received GF particles in the aqueous dispersant (HPC/Sol–SDS) solutions first. The resultant GF pre-suspensions were transferred to the holding tank of a Microcer wet stirred media mill (WSMM) (Netzsch Fine Particle Technology, LLC, Exton, PA, USA) with 80 mL milling chamber (Fig. 1a). Milling conditions were adopted from our prior work on WSMM [63,64]. Milling chamber was filled with 50 mL zirconia beads, and to hold the beads in the chamber a screen with 200 μm opening was used at the outlet of the chamber. The pre-suspension was recirculated through the chamber at a rate of 126 mL/min via a peristaltic pump and was milled at a rotor speed of 3200 rpm for 64 min. A portion of each suspension was separated in a vial and stored for 7-days at 8 °C to assess the short-term physical stability. Also, the milled suspensions were refrigerated at 8 °C for overnight before spray drying.

To prepare the solution-based (S) feeds, a mixture of acetone–water was purposefully selected to dissolve all components of the formulation (Fig. 1b). To ensure a *head-to-head* comparison of the nanocomposites with ASDs, the formulations of the solution-based (S) feeds are kept identical to those of the suspension-based (W) feeds. 40 mL of deionized water was added to 200 mL acetone to prepare a total of 240 mL solvent mixture. After dissolving the drug–polymer–surfactant into the binary solvent mixture using a magnetic stirrer, the solutions were sonicated for 30 min before feeding to the spray dryer.

Using a spray dryer (4 M8-Trix, Procept, Zelzate, Belgium) having a co-current flow set-up (Fig. 1c), GF suspensions and drug–polymer solutions were dried. The total length and the diameter of the spray dryer are 1.59 m and 0.15 m, respectively. To ensure complete drying, inlet temperature was selected above the boiling temperature of the respective pure liquids. Drying air at 120 °C flowing at 0.37–0.40 m^3/min and drying air at 75 °C flowing at rate of 0.27–0.30 m^3/min were fed co-currently at the top of the dryer column to dry W feeds and S feeds (see Table 2), respectively. 200 g suspension/solution of each formulation was sprayed at 2.0 g/min rate using a peristaltic pump (Make-it-EZ, Creates, Zelzate, Belgium). A cyclone separator was used to separate the dried particles from the outlet stream into a glass jar. Atomizing air pressure of 2.0 bar, a bi-fluidic nozzle with tip diameter of 0.6 mm, and cyclone pressure of 55–60 mbar were selected based on prior experience [27] and exploratory experiments. The dried particles obtained from the collection jar were transferred into double plastic bags and stored in a vacuum-desiccator at room temperature for further characterization.

2.3. Characterization techniques

2.3.1. Particle sizing

Drug particle size distributions (PSDs) in the suspensions were measured by laser diffraction (LS 13 320, Beckman Coulter, Miami, FL) based on Mie scattering theory following the procedure described in ref. [64] at various times: right after milling, after 1-day and 7-day storage at 8 °C to in a refrigerator. The intensity was maintained between 40 and 50% while the obscuration was maintained below 8.0% for all measurements. Refractive index values are 1.65 for GF (drug) and 1.33 for deionized water (medium). Before each measurement, a 2.0 mL suspension sample was dispersed into 5.0 mL of the respective stabilizer solution using a vortex mixer (Fisher Scientific Digital Vortex Mixer, Model No: 945415, Pittsburgh, PA) at 1500 rpm for one min prior to each measurement.

The particle sizes of the spray-dried powders and as-received GF were measured by a Rodos/Helos laser diffraction system (Sympatec, NJ, USA) based on Fraunhofer theory following the procedure described in ref. [31]. About 1 g of the powder sample was placed on top of the sample chute of the Rodos dispersing system and the sample chute was vibrated at a 100% setting, and 0.1 bar dispersion pressure was used to suck in the falling powder through the sample cell of the laser diffraction system. For morphological analysis, spray-dried particles were placed on a glass slide and observed by Axio Scope.A1 polarized light microscope (PLM, Carl Zeiss Microscopy GmbH, Göttingen, Germany).

2.3.2. Solid state characterization and drug–polymer interactions

To analyze the crystallinity of the as-received GF, HPC, Sol, SDS,

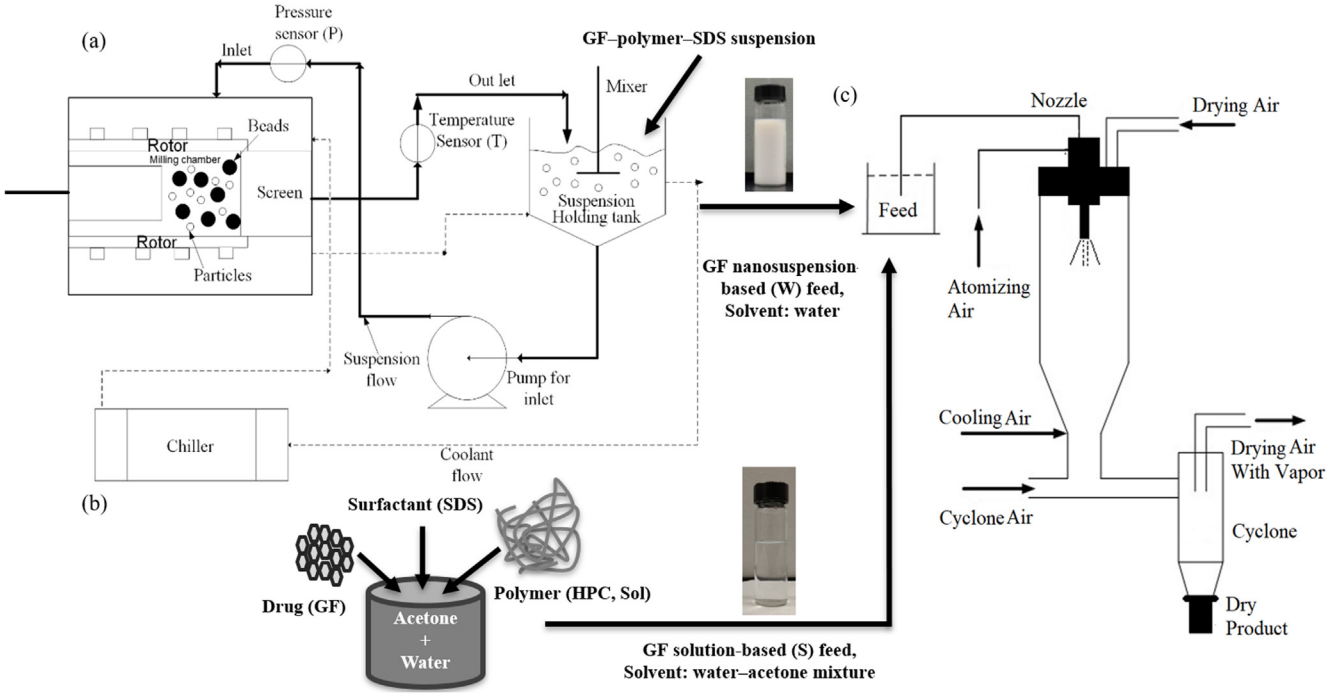

Fig. 1. Schematic illustration of the process setup: (a) wet-stirred media milling (WSMM) of drug in aqueous solution of polymer–surfactant for the preparation of the drug nanosuspension-based (W) feed, (b) mixing of drug, polymer, and surfactant in acetone–water mixture for the preparation of the drug solution-based (S) feed, and (c) co-current spray drying of each feed separately. Diagrams are not drawn to scale.

Table 2
Formulations of the suspension-based (W) feeds and solution-based (S) feeds used in spray drying.

Formulation[a]	GF (% w/v)[b]	Polymer (% w/v)[b]	SDS (% w/v)[b]	Water (mL)	Acetone (mL)
W-Sol-1:3	2.5	7.5	0.125	240	0
W-Sol-1:1	2.5	2.5	0.125	240	0
W-Sol-3:1	2.5	0.8	0.125	240	0
W-HPC-1:3	2.5	7.5	0.125	240	0
W-HPC-1:1	2.5	2.5	0.125	240	0
S-Sol-1:3	2.5	7.5	0.125	40	200
S-Sol-1:1	2.5	2.5	0.125	40	200
S-HPC-1:3	2.5	7.5	0.125	40	200
S-HPC-1:1	2.5	2.5	0.125	40	200

[a] S denotes solution-based feed; W denotes nanosuspension-based feed; Sol denotes Soluplus; the ratios refer to the drug:polymer mass ratios. All formulations have 0.125% w/v SDS.

[b] % w/v with respect to the total volume (240 mL) of the liquid (water/solvent).

spray-dried powders, and physical mixtures of GF–polymer–SDS (same formulation as stated in Table 2), X-ray powder diffraction (XRPD) (PANanalytical, Westborough, MA, USA), provided with Cu K_α radiation (λ = 1.5406 Å) was used. The samples were scanned at a rate of 0.165 s^{-1} for 2θ ranging from 5° to 40°. The total area under three distinct, non-overlapping peaks of GF at characteristic diffraction angles of 13.2°, 14.6°, and 16.5° was calculated for both the physical mixtures and the spray-dried powders using the equipment's HighScore Plus software, which was then used to estimate the crystallinity.

Differential scanning calorimetry (DSC) of the as-received GF, Sol, HPC, physical mixtures of GF–polymer–SDS, and spray-dried powders was performed using a Mettler-Toledo polymer analyzer (PolyDSC, Columbus, OH, USA) with integrated STARe 10 software. ~6.0–7.0 mg powder sample was placed in an aluminum pan with a hole in the lid and loaded into the DSC machine. As-received GF was heated at a rate of 10 °C/min from 25 °C to 250 °C. All other samples were heated from 25 °C to 70 °C and the temperature was held for 2 min at 70 °C, then cooled back to 25 °C to remove any residual solvent in the sample. In the final step, the samples were heated from 25 °C to 250 °C at 10 °C/min. Nitrogen gas was used as the purge gas and protective gas at a flow rate of 50 mL/min and 150 mL/min, respectively. Thermogravimetric analysis (TGA) was performed to measure the residual water/solvent content using a TGA/DSC1/SF Stare system (Mettler Toledo, Inc., Columbus, OH). ~6.0–7.0 mg of each spray-dried sample was placed in a ceramic crucible and heated from 25 °C to 150 °C at a heating rate of 10 °C/min under nitrogen flow.

Raman spectroscopy was conducted using a Fergie Imaging Spectrometer System (Princeton Instruments, Trenton, NJ) with a 500-mW external diode laser processing at 785 nm wavelength. Data acquisition time for all spectra was 15 s per scanned spectrum (100–1800 cm^{-1}) and each spectrum acquired was averaged over two scans. The data was presented for the range of 1550–1800 cm^{-1} wavenumber.

2.3.3. Characterization of drug recrystallization

To elucidate the role of drying rate on drug recrystallization during drying, a droplet of 20 µL of the solution prepared for the solution-based (S) feed was put onto a hot glass slide at 75 °C and kept for drying in quiescent air. After about one min drying, the slides were placed under the polarized light microscope (PLM) to observe if any drug recrystallization occurred. To elucidate GF recrystallization in the presence of water, a small portion of the spray-dried powders prepared using the solution-based (S) feed (S-HPC-1:3 and S-Sol-1:3) was gently pressed to form a loose compact, which was then mounted onto a microscopic glass slide, and placed under the PLM. 20 µL of deionized water was added to the sample and the PLM images were captured at 0, 1, 2, and 5 min from the moment of water addition.

2.3.4. Study of nanoparticle recovery from the nanocomposites

Aqueous redispersion of the nanocomposites was performed following a previously established method [31,46]. About 0.5 g of the spray-dried powders prepared using the nanosuspension-based (W) feeds was dispersed in 30 mL of deionized water inside a 60 mL beaker

and stirred at 500 rpm for 60 min with a paddle-stirrer (CAT R18, Scientific Instrument Center Limited, Winchester, UK). ~1.0 mL aliquot of redispersed sample was taken at 2, 10 and 60 min while stirring, and particle size was measured using laser diffraction (LS 13 320, Beckman Coulter, Miami, FL). At the same collection times, a droplet of each redispersed sample was taken and dried immediately by dropping on a preheated glass slide on a hot plate at 100 °C. After drying, the PLM was used to capture images of the redispersed particles. The details of the methods and results are presented in Section S.1 of *Supplementary Material*.

2.3.5. Drug content and dissolution performance of the spray-dried powders

The drug content in the dried powders varied based on the drug:-polymer mass ratios. To measure the actual drug content in the spray-dried powders, an assay testing was performed by dissolving 100 mg of the sample powders in 20 mL methanol under 30 min of sonication, followed by overnight storage to ensure complete solubilization of the GF particles. An aliquot of 100 µL was taken from the GF solution and diluted up to 10 mL using methanol. The absorbance of the samples was measured at 292 nm using UV spectrophotometer (Agilent, Santa Clara, CA, USA), and the drug concentration was calculated from a pre-established calibration curve. Six replicates were tested for each formulation to calculate mean drug content along with the relative standard deviation (RSD).

Drug release from the spray-dried powders and various physical mixtures (PMs) prepared by blending was determined via a Distek 2100C dissolution tester (North Brunswick, NJ, USA), following the USP II paddle method. 1000 mL deionized water at 37 °C was stirred at 50 rpm paddle speed. Deionized water was selected as the dissolution medium as it provided good discrimination of different GF nanocomposites and GF ASDs in previous studies [17,26,39] and allows for supersaturation of the HyNASDs/nanocomposites as well as ASDs in this study for comparative analysis. Spray-dried powder samples containing 100 mg GF (above the thermodynamic solubility of as-received GF particles) were weighed and added to the dissolution medium and 4 mL samples were taken out manually at 1, 2, 5, 10, 20, 30, 60, 120, 180, and 210 min. These aliquots were filtered through 0.1 µm PVDF membrane-type syringe filter before UV-spectroscopy measurements (similar to refs. [17,26]). The filtered samples were diluted with 37 °C deionized water at a ratio of 1–5 before UV measurement. Dissolved GF amount was measured by UV spectroscopy at 296 nm wavelength and calculated using a pre-established calibration curve. Deionized water was used as the blank before UV measurement and six replicates of each sample were performed. In this paper, relative % supersaturation is reported based on GF concentration at 210 min and thermodynamic solubility of as-received GF particles, unless otherwise indicated.

2.3.6. Supersaturation maintenance ability of the polymers

The supersaturation maintenance ability of HPC/Sol was examined in a separate desupersaturation test (similar to ref. [65]). A concentrated solution of GF in acetone was prepared by dissolving 100 mg of as-received GF in 20 mL acetone. This solution was subsequently added to 1000 mL of pre-dissolved HPC–SDS/Sol–SDS solution with 100 µg/mL and 300 µg/mL polymer concentration, which maintained 1:1 and 1:3 drug:polymer mass ratio, respectively, in the USP II paddle type dissolution tester. The addition resulted in 92–99 µg/mL supersaturated solutions of GF initially, and any subsequent desupersaturation during the following 210 min was tracked via GF concentration measurements. The experimental conditions and concentration measurement were identical to those in the dissolution test. All measurements were carried out in triplicate.

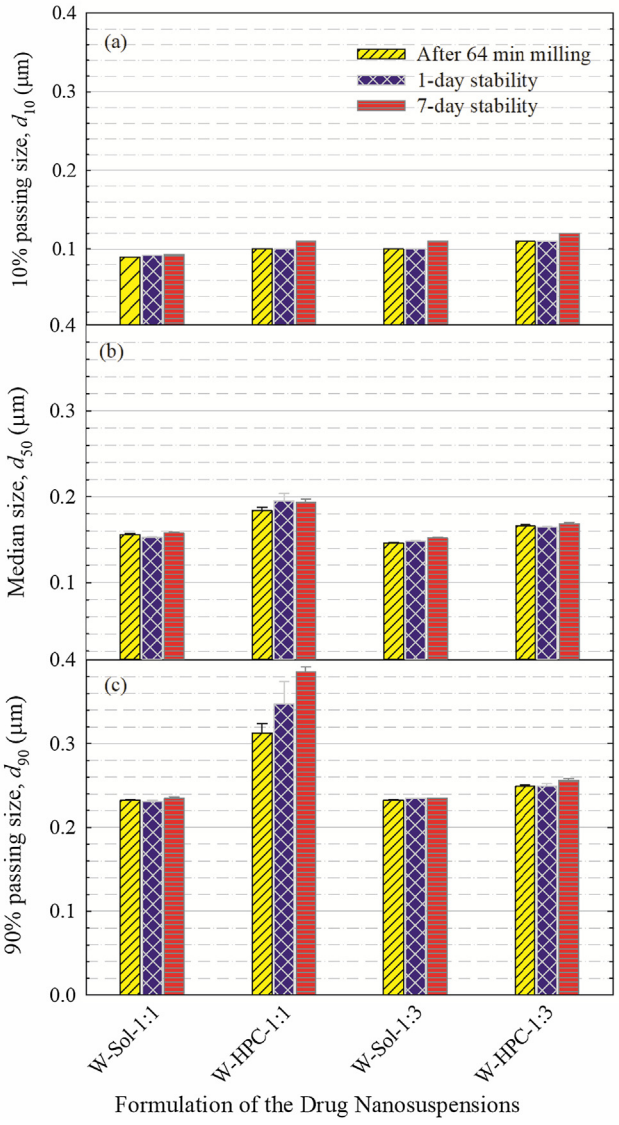

Fig. 2. Volume-based particle size statistics of the milled GF suspensions with 1:1 and 1:3 GF:polymer mass ratios after milling (64 min) as well as 1-day storage and 7-day storage at 8 °C: (a) 10% cumulative passing size d_{10}, (b) median particle size d_{50} and (c) 90% cumulative passing size d_{90}. All suspensions have 2.5% w/v GF and 0.125% w/v SDS.

3. Results and discussion

3.1. Properties of GF nanosuspensions prepared via wet stirred media milling

Four different GF suspensions were wet media milled using HPC/Sol at 1:1 and 1:3 drug:polymer mass ratios in the presence of SDS. The median particle size d_{50} and 90% passing size d_{90} of the final milled suspensions (after 64 min), after 1-day and 7-day storage are presented in Fig. 2. Unless properly stabilized, GF nanoparticles severely aggregate in aqueous suspensions, forming micron-sized particles [31]. The wet-milling of as-received (micronized) GF particles with d_{10}: 3.04 ± 0.1 µm, d_{50}: 10.0 ± 0.17 µm and d_{90}: 28.2 ± 0.14 µm (see the full the particle size distribution in Fig. S3 of *Supplementary Material*) yielded nanosuspensions with d_{50} in the range of 0.14–0.19 µm. The small changes in d_{50} and d_{90} during the 7-day storage suggest that the suspensions did not undergo drastic aggregation/growth during milling and storage. On the other hand, an increase in HPC concentration led to smaller aggregates and finer sizes. In a previous study, HPC–SDS was

Table 3
Particle size statistics of the spray-dried powders and their drug content.

Formulation[a]	Particle size statistics of the spray-dried particles (μm)			Actual drug content, RSD (% w/w, %)	Theoretical drug content (% w/w)
	d_{10} ± SD	d_{50} ± SD	d_{90} ± SD		
W-Sol-1:3	9.29 ± 0.1	19.0 ± 0.1	33.6 ± 0.1	21.2, 1.50	24.7
W-Sol-1:1	4.48 ± 0.1	10.1 ± 0.1	21.9 ± 0.2	42.0, 1.73	48.8
W-Sol-3:1	1.66 ± 0.1	6.89 ± 0.3	15.3 ± 0.4	64.4, 0.51	72.3
W-HPC-1:3	6.37 ± 0.1	16.5 ± 0.6	40.0 ± 0.1	22.3, 3.14	24.7
W-HPC-1:1	5.24 ± 0.1	12.9 ± 0.1	34.2 ± 0.1	42.5, 2.83	48.8
S-Sol-1:3	4.11 ± 0.0	12.3 ± 0.0	33.2 ± 0.1	21.5, 2.02	24.7
S-Sol-1:1	5.03 ± 0.1	11.0 ± 0.1	20.2 ± 0.0	42.3, 2.21	48.8
S-HPC-1:3	6.48 ± 0.0	15.8 ± 0.6	31.3 ± 1.0	24.4, 2.56	24.7
S-HPC-1:1	7.05 ± 0.2	13.0 ± 0.9	26.9 ± 0.8	41.7, 0.73	48.8

[a] S denotes solution-based feed, W denotes nanosuspension-based feed, Sol denotes Soluplus; the ratios refer to the drug:polymer mass ratios. All formulations have 0.125% w/v SDS.

reported to have synergistic stabilizing effect on GF suspensions during milling and storage [66] and stabilized multiple BCS Class II drug nanosuspensions [64]. HPC and Sol imparted steric stabilization by adsorbing on drug nanoparticles [66,67], while the anionic surfactant (SDS) enhanced GF wettability/deaggregation and helped to stabilize the GF nanosuspensions via electrostatic repulsion [64,66].

3.2. Size, morphology, and drug–moisture content of the spray-dried powders

Drug nanosuspension-based (W) feeds produced by WSMM and drug–polymer solution-based (S) feeds with identical formulations were spray-dried separately. The residence time in the spray dryer was short, i.e., 4.0 s and 5.0 s, for W feeds and S feeds, respectively. Despite the relatively short residence time, the spray-dried powders were completely dried, as indicated by the TGA, which shows weight loss of ~2.0% for the samples. The extremely large surface area generated by atomization of the feed coupled with the fast convective heat–mass transfer at high air temperature enabled fast drying of the droplets. The mean (actual) drug content of the spray-dried powders was higher for feeds with higher drug:polymer mass ratio (Table 3). RSD values were below 6%: 0.73–3.14%, which signifies pharmaceutically acceptable content uniformity. The slightly lower drug content as compared with the theoretical value can be attributed to preferential drug loss during handling/transfer after milling, poor separation of finer particles in the cyclone separator of the spray dryer, and presence of the residual moisture after drying [27,46]. The median sizes of the spray-dried powders were measured to be in the range of 6.89–19.0 μm and 11.0–15.8 μm (Table 3) for W feeds and S feeds, respectively. An increase in polymer loading led to formation of coarser particles due to increase in total solids loading and higher viscosity of the feed [45,46,50]. The microscopic images (Fig. 3) illustrate that spray-dried particles have rounded–donut shapes, and their sizes are in rough agreement with the ranges mentioned in Table 3.

3.3. Formation of drug nanocomposites/HyNASDs vs. ASDs upon spray drying

The solid state of GF in the spray-dried powders was investigated via XRPD (see Fig. 4) and DSC (see Fig. 5). Table 4 presents the summary of DSC thermal events and estimated crystallinity via XRPD. X-ray diffractograms depict that as-received GF exhibited intense peak characteristics of a crystalline material, whereas HPC/Sol exhibited halo pattern indicating amorphous structure (Fig. 4a). The physical mixtures (PMs), prepared by blending, exhibited peaks at the same diffraction angles as those of as-received GF, albeit with reduced peak intensity (Fig. 4b and c), which can be attributed to the dilution and surface coverage of GF microparticles with HPC/Sol, and the reduction is more discernible with increasing polymer concentration. The peaks observed between 5°–10° in the physical mixtures (PMs) correspond to the main characteristic peaks of SDS, which is also crystalline in nature. The main characteristic peaks of SDS are at 5.6°, 6.8°, and 8.3° (refer to Fig. S4 of *Supplementary Material*; the SDS diffractogram was excluded from Fig. 4 for proper scaling of GF peaks).

In general, similar XRPD diffractograms to those of the PMs were observed for the spray-dried powders prepared using the suspension-based (W) feeds confirming that spray-drying of W feeds led to formation of nanocomposites that are mostly crystalline (Fig. 4b and c). The characteristics peaks of SDS present in the PMs were absent in the diffractograms of the spray-dried powders as small amount of SDS was most likely molecularly dispersed in the polymeric matrix of the spray-dried powders. Interestingly, the diffractograms of the spray-dried powders with W feeds especially those with higher polymer loading (lower GF:polymer ratio) show clear peak broadening and peak intensity reduction as compared with those of PMs, beyond the aforementioned dilution effect. Surprisingly, wet milling followed by spray-drying led to reduction of crystallinity and formation of notable (~5–20%) amorphous drug (see Table 4). To the best knowledge of the authors, this level of amorphous content in drug nanocomposites is not common. It is well-established that wet media milling does not cause any detectable amorphization of as-received GF, in the absence of stabilizers, due to plasticization effect of water [68]. In the presence of high polymer loading in the nanosuspensions here, however, amorphization of GF took place during the spray drying.

Table 4 shows that despite being largely crystalline, the amorphous content in the spray-dried powders prepared via nanosuspension-based (W) feeds increased upon an increase in the polymer loading in the nanosuspensions. Moreover, higher amorphous content was observed in the Sol formulations than in the HPC formulations at the same drug:-polymer mass ratio. These findings suggest that amorphous GF was formed due to GF–polymer molecular interactions and/or solubilization of the surface layer of nanoparticles by the polymer during the spray-drying. It is likely that presence of GF nanoparticles with large surface area could have facilitated the formation of amorphous content around the GF nanoparticles. In other words, the polymeric matrix of the spray-dried particles encapsulates drug nanocrystals, surrounded by a layer of amorphous GF ASD in the polymeric matrix (see Fig. 6b). Formation of amorphous content upon drying of drug nanosuspensions was first observed by [69], albeit to a much lower extent; however, the impact of such amorphous content on drug release from the nanocomposites has not been studied at all. As the dissolution tests will reveal below, despite being largely crystalline, these nanocomposites with high polymer loading (low drug:polymer ratio) allow for much higher drug supersaturation than traditional nanocomposites; hence, we refer to them as HyNASDs. The higher amorphous content in the Sol than in the HPC formulations could be related to the stronger molecular interactions of Sol with GF than HPC with GF and GF–Sol miscibility. It is suggested that if the solubility parameter difference between a drug and polymer

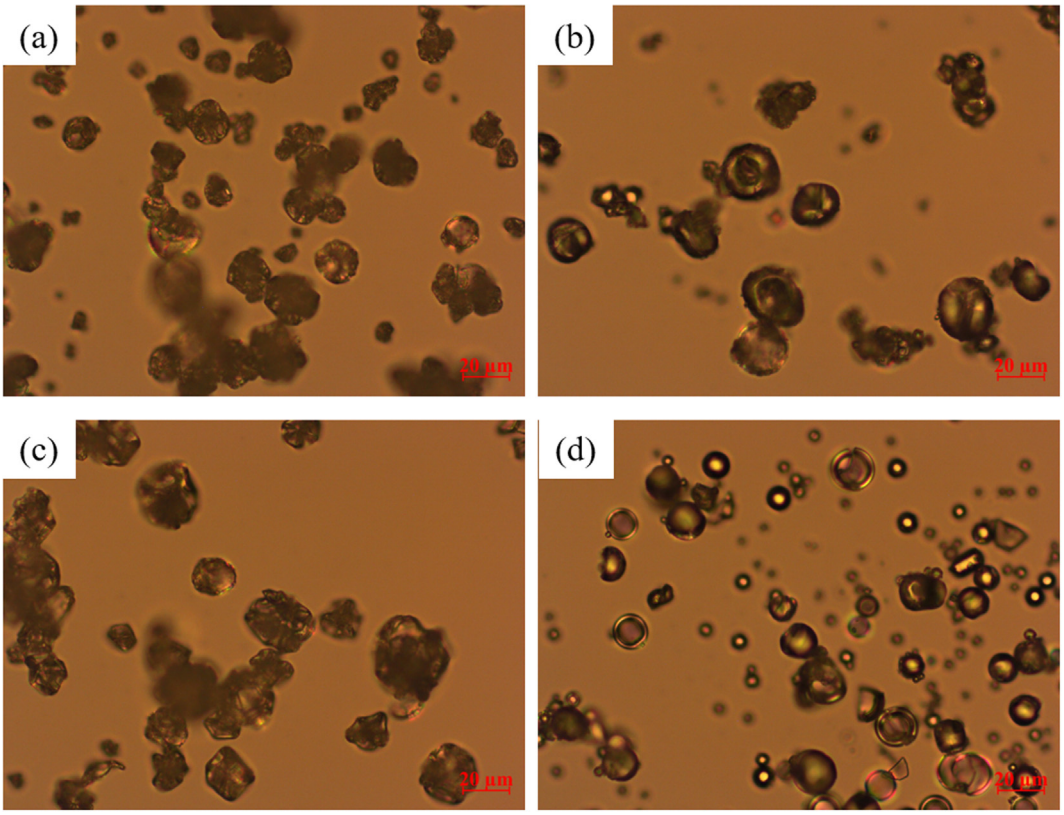

Fig. 3. Polarized light microscope images of the spray-dried particles prepared using the GF nanosuspension-based (W) feed and the GF solution-based (S) feed with 1:3 GF:polymer mass ratios: (a) W-HPC-1:3, (b) S-HPC-1:3, (c) W-Sol-1:3, and (d) S-Sol-1:3. All images were taken at 50X magnification (scale bar: 20 μm).

is < 7.0 $MPa^{1/2}$, they are likely to be miscible; if the difference is > 10 $MPa^{1/2}$, they are considered immiscible [70,71]. The solubility parameters of GF, HPC, and Sol are 12.2 [72], 24.0 [73], and 19.4 [74] $MPa^{1/2}$, respectively. The solubility parameter differences between GF–Sol and GF–HPC are 7.2 and 11.8 $MPa^{1/2}$, respectively, which suggests that GF–Sol is borderline miscible (or at least partially miscible), whereas GF–HPC is most likely immiscible. While being useful, the solubility parameters do not account for all drug–polymer interactions such as contributions from hydrogen bonding, hydrophobic interactions, etc., and hence should be used with caution as rough estimates of drug–polymer miscibility.

XRPD diffractograms (Fig. 4b and 4c) of the spray-dried powders prepared using the solution-based (S) feeds showed halo pattern instead of any characteristic diffraction peaks of GF (except S-HPC-1:1). These halo patterns confirm that amorphous GF dispersed molecularly into the polymer matrix forming amorphous solid dispersions (ASDs). Despite the immiscibility of HPC with GF, fast drying of acetone–water in 1:3 GF–HPC solution led to molecular dispersion and arrested amorphous GF in the HPC matrix kinetically. On the other hand, the peaks in the XRPD diffractogram of S-HPC-1:1 and 6.5% crystalline GF could be explained by the insufficient HPC concentration to ensure complete dispersion of GF molecules in the polymer matrix; hence, recrystallization of GF during spray-drying occurred.

The DSC thermograms in Fig. 5a show an endothermic peak associated with melting of as-received GF, with a T_m of 220.1 °C and ΔH_f of 101.8 J/g; a glass transition for Sol (amorphous) at 72.4 °C, and a slight endothermic event around 170–200 °C for HPC likely due to the melting of the small crystalline domain of largely amorphous HPC [75] (crystallinity was undetectable by XRPD). The T_g of HPC could not be measured (in the range of –25 to 0 °C [75]) due to limitation of our equipment. For spray-dried powders prepared using solution-based (S) feeds, a single T_g was observed for all the formulations confirming the formation of molecular level dispersion [76,77] (see Table 4 and ASD schematic in Fig. 6c). While S-Sol-1:3 exhibited only a glass transition, all other ASDs exhibited a glass transition followed by an exothermic event due to re-crystallization of amorphous GF followed by the melting of the recrystallized GF (Fig. 5b and c). The (absolute value) enthalpy of recrystallization was lower for Sol than for HPC formulations and was lower when a higher polymer loading was used (in line with other studies e.g. [76]). Recrystallization occurred during the heating step of DSC scan because above T_g amorphous drug molecules and amorphous polymer had higher mobility, leading to GF recrystallization. Due to stronger molecular interactions and miscibility of Sol with GF, S-Sol-1:3 with high Sol loading was able to inhibit recrystallization even at high temperatures during the DSC scan.

The spray-dried powders prepared using the suspension-based (W) feeds, i.e., the nanocomposites including HyNASDs, exhibited a melting endotherm only (Fig. 5b and 5c). The T_m and fusion enthalpy ΔH_f of these spray-dried powders were lower than those of the respective physical mixtures (Table 4). Moreover, higher polymer loading (1:3 vs. 1:1 W formulations) led to lower T_m and ΔH_f, similar to the lower peaks and crystallinity in XRPD. The observed reduction in T_m and ΔH_f of HyNASDs, as compared with the physical mixtures, may be partly attributed to defect formation and accumulation during milling. However, only a slight reduction in T_m and ΔH_f occurred upon wet media milling of GF without stabilizers [68]. Hence, the reduction in T_m and ΔH_f was mostly attributed to amorphization of GF on the surface of the drug nanocrystals [69] or its solubilization in the polymer upon spray-drying as well as the solubilization during the DSC scan. Compared with the thermogram of as-received GF, the thermograms of the physical mixtures also show a significant reduction of T_m and ΔH_f, which can be explained by the solubilization of GF in molten polymer at high temperatures during the DSC scan. Finally, the lower T_m and ΔH_f of the W-Sol formulations than those for the W-HPC formulations could again be explained by the higher miscibility and stronger molecular interaction of Sol with GF than HPC with GF.

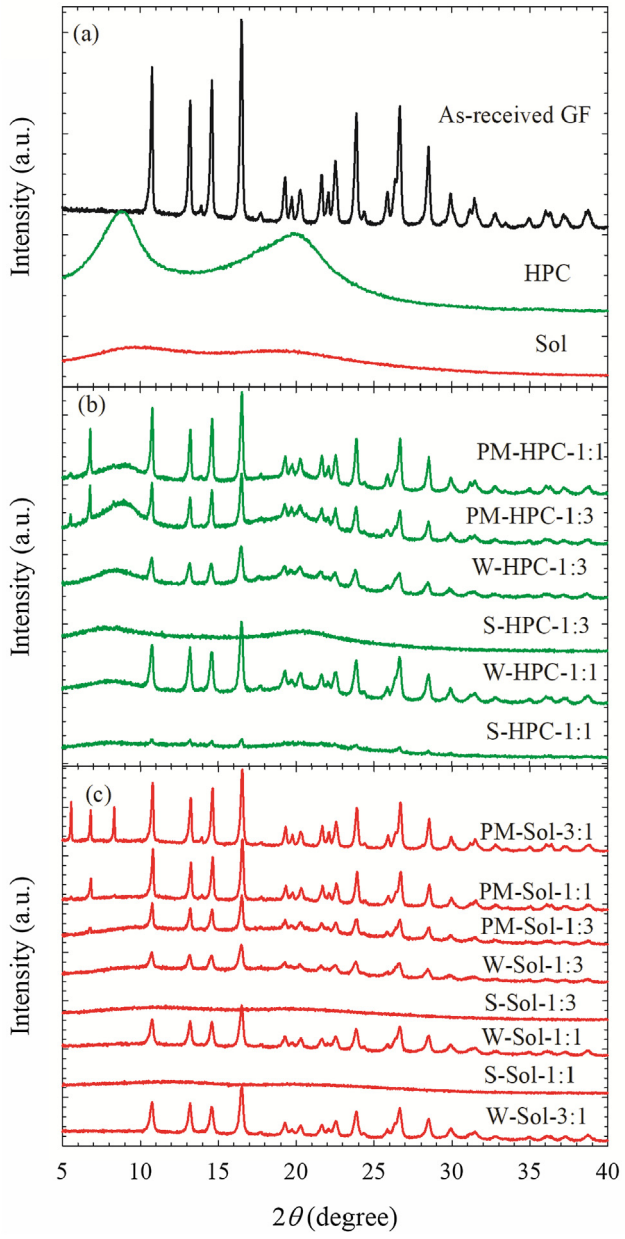

Fig. 4. X-ray diffractograms of as-received GF, HPC, and Sol (a); physical mixtures (PMs) of GF–polymer–SDS and the spray-dried powders prepared using the GF nanosuspension-based (W) feed and GF solution-based (S) feed with various GF:polymer mass ratios: HPC as the polymer (b) and Sol as the polymer (c).

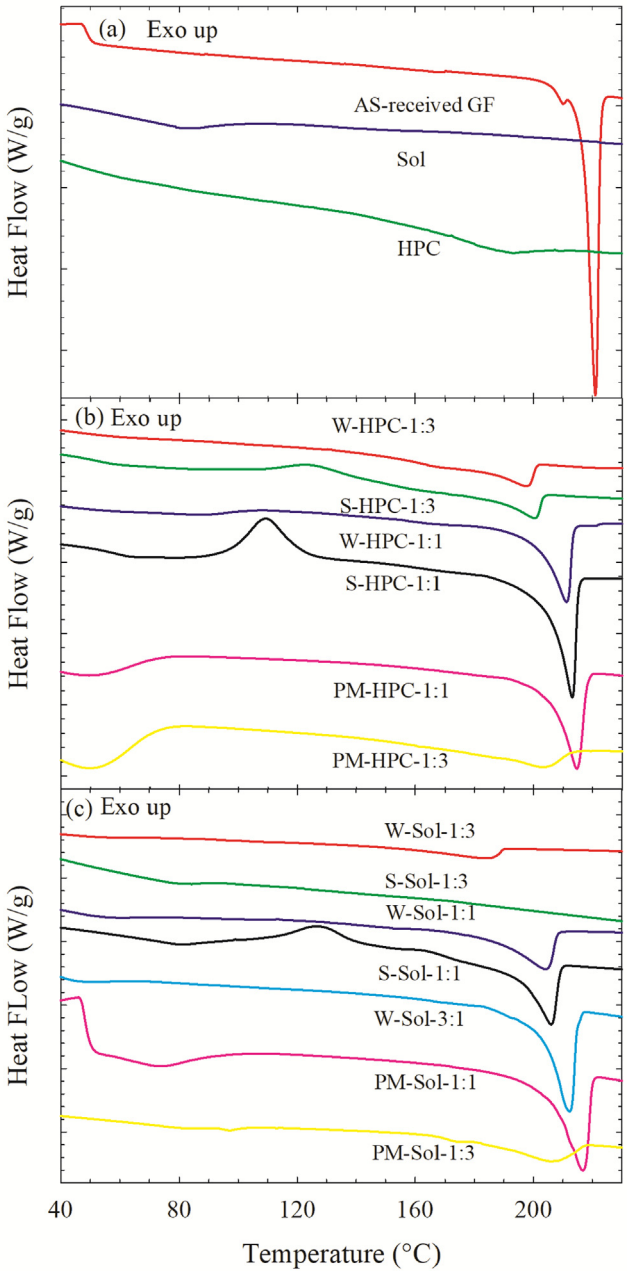

Fig. 5. DSC thermograms of as-received GF, HPC, and Sol (a); physical mixtures (PMs) of GF–polymer–SDS and the spray-dried powders prepared using the GF nanosuspension-based (W) feed and GF solution-based (S) feed with various GF:polymer mass ratios: HPC as the polymer (b) and Sol as the polymer (c).

The observed Raman lines in Fig. 7a for as-received GF and PMs of GF are largely in agreement with Fourier transform Raman data of ref. [78] and Raman data of ref. [79] for crystalline GF. The Raman spectra of S-Sol-1:3 (Fig. 7c) show that the GF line at 1606 cm^{-1} disappeared, and the lines at other characteristic frequencies shifted to new positions that are characteristic of amorphous GF, e.g., the line shift from 1712 to 1715 cm^{-1} (see Zarow et al. [79]), signifying formation of amorphous GF and strong molecular interactions between GF and Sol in the ASD. While the GF line at 1606 cm^{-1} disappeared in the Raman spectra of S-HPC-1:3 (Fig. 7b), the shifts in other lines were subtler than those for the Raman spectra of S-Sol-1:3, which could suggest stronger molecular interactions between GF and Sol than GF and HPC. While the W-Sol-1:3 and W-HPC-1:3 powders (HyNASDs) did not show disappearance of lines or line shifts, unlike S-Sol-1:3 and S-HPC-1:3 powders (ASDs), their spectra clearly show broadening of the characteristic GF lines and peak intensity reduction as compared with the spectra of the respective PMs due to GF–polymer interactions and presence of amorphous domains in these powders. In contrast, the spectra of W-Sol-3:1 (nanocomposite), having 1/9th of Sol content compared with W-Sol-1:3, did not show as much line broadening compared to the spectra of its respective PM.

The XRPD, DSC, and Raman spectroscopy results overall suggest that spray-drying of GF–polymer solutions (S feeds) led to formation of ASDs, whereas spray-drying of GF–polymer nanosuspensions (W feeds) led to formation of drug nanocomposites/HyNASDs. Although a hard and crisp distinction between traditional nanocomposites and HyNASDs is not intended here, HyNASDs appear to have notable amorphous content (> %10 in XRPD) and/or exhibit significant T_m depression–ΔH_f reduction and GF Raman peak broadening as compared with the

Table 4
Characteristic temperatures–enthalpy values obtained from DSC thermograms and crystallinity estimated from XRPD diffractograms.

Formulation[a]	T_g (°C)[a,b]	T_{rc} (°C)[a,b]	ΔH_{rc} (J/g)[a,b]	T_m (°C)[a,b]	ΔH_f (J/g)[a,b]	Crystallinity (%)[b]
S-HPC-1:1	58.9	109	–20.0	213	40.6	6.5
W-HPC-1:1	ND	ND	ND	211	28.7	95.5
S-HPC-1:3	57.7	124	–1.71	200	10.5	ND
W-HPC-1:3	ND	ND	ND	198	12.7	86.5
W-Sol-3:1	ND	ND	ND	212	47.0	92.1
S-Sol-1:1	74.6	127	–9.26	206	25.4	ND
W-Sol-1:1	ND	ND	ND	204	22.7	86.3
S-Sol-1:3	80.0	ND	ND	ND	ND	ND
W-Sol-1:3	ND	ND	ND	186	7.37	81.3

[a] S denotes solution-based feed, W denotes nanosuspension-based feed, Sol denotes Soluplus; the ratios refer to the drug:polymer mass ratios. All formulations have 0.125% w/v SDS. Other symbols: T_g, T_{rc}, and T_m stand for temperature for glass transition, recrystallization transition, and melting point, respectively, while ΔH_{rc} and ΔH_f respectively stand for recrystallization enthalpy and fusion enthalpy.
[b] ND: not detected.

respective physical mixtures. As a general observation, we note that spray-drying a drug nanosuspension with a lower drug:polymer mass ratio (1:1, 1:3) than typically used (see e.g. Table 1) and the use of a miscible polymer, i.e., Sol, that interacts with the drug nanoparticles strongly and potentially solubilizes them during the spray drying favor the formation of HyNASDs vs. nanocomposites (W-Sol-1:3 vs. W-Sol-3:1). Moreover, as will be shown in Section 3.5, nanocomposites and HyNASDs may behave quite differently in their functional responses such as drug release *in vitro*.

3.4. Impact of drying rate and polymers on inhibition of GF recrystallization

In the solution-based (S) feeds, GF, polymer, and SDS were completely dissolved in acetone–water mixture, which allowed molecular level interaction in the solution before spray drying. Due to fast evaporation of the solvents in the spray dryer, viscosity increases rapidly causing entrapment of the drug molecules in the polymer matrices, which appears to have retarded phase separation even in the case of GF–HPC (relatively immiscible) and enables the ASD formation. In the nanosuspension-based (W) feeds, GF exists as nanocrystalline particles while polymer and SDS were dissolved in water. However, due to large surface area of GF nanocrystals and presence of relatively high polymer loading (1:1 and 1:3 GF:polymer), GF was partially solubilized or molecularly dispersed, especially in Sol, as the evaporation proceeds, leading to formation of GF molecularly dispersed in the polymer matrix surrounding the GF nanocrystals (refer to Fig. 6b).

To demonstrate the criticality of drying rate and drug–polymer interactions/miscibility, we have devised a slower drying method: a single droplet of GF–HPC–SDS solution on a heated glass slide at 75 °C, same temperature as that of hot air in the spray-drying. However, the droplet was dried in quiescent air, which makes external mass transfer of solvent vapor in air controlling the evaporation rate, making drying slower compared to spray drying. The drying took less than 40 s, whereas the drying occurred less than ~5 s in the spray dryer. The PLM images in Fig. 8 illustrate that GF crystals formed during the slow drying of all solutions. On the other hand, the drying of S-Sol-1:3 solution yielded few small crystals, whereas that of S-Sol-1:1 solution yielded significant number of needle-shaped crystals. The extent of recrystallization was much higher in HPC than in Sol. HPC could not inhibit the nucleation/crystal growth of GF from the supersaturated solution as evaporation proceeded during the spray-drying. Since only S-HPC-1:1 spray-dried powder had 6.5% crystalline GF and others solution-based (S) spray-dried samples did not have detectable GF crystals, it is concluded that the relatively fast evaporation during the spray drying enabled ASD formation.

It is known that the phase separation and recrystallization involve diffusion of drug molecules and nucleation, both of which require molecular mobility and can be restricted by polymer molecules as inhibitor [55]. Strong drug–polymer interactions can reduce the molecular mobility and delay crystallization onset time and the extent of crystallization [80]. This is in line with earlier work, e.g., [81], where the recrystallization time of nifedipine increased with an increase in polymer (PVP) concentration. To gain additional insights into the GF recrystallization inhibition capability of Sol/HPC in solutions,

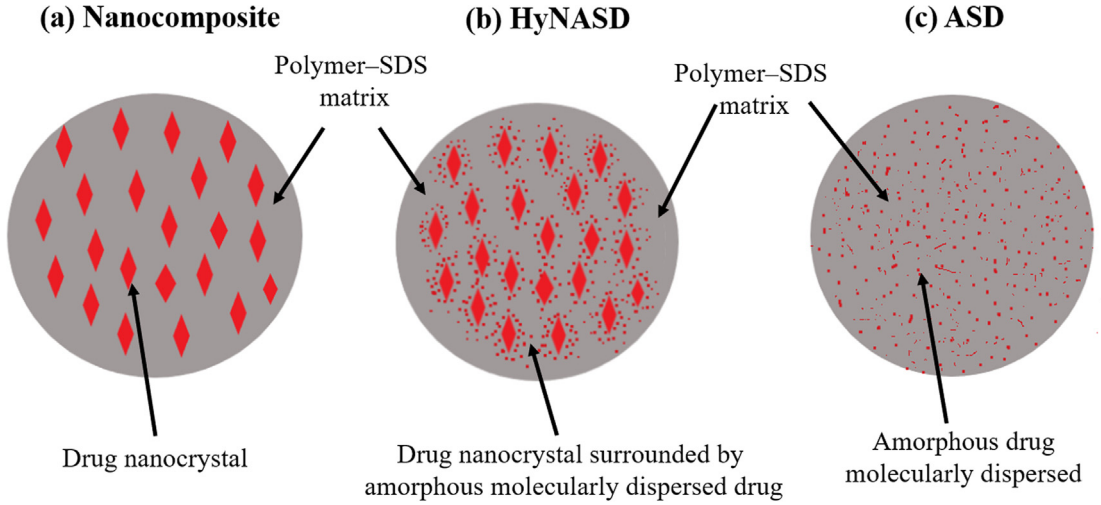

Fig. 6. Schematic illustration of the solid state of the drug (GF) in GF nanocomposite (a), GF hybrid nanocrystal–amorphous solid dispersion (HyNASD) (b), and GF amorphous solid dispersion (ASD) (c). Figure is not drawn to scale.

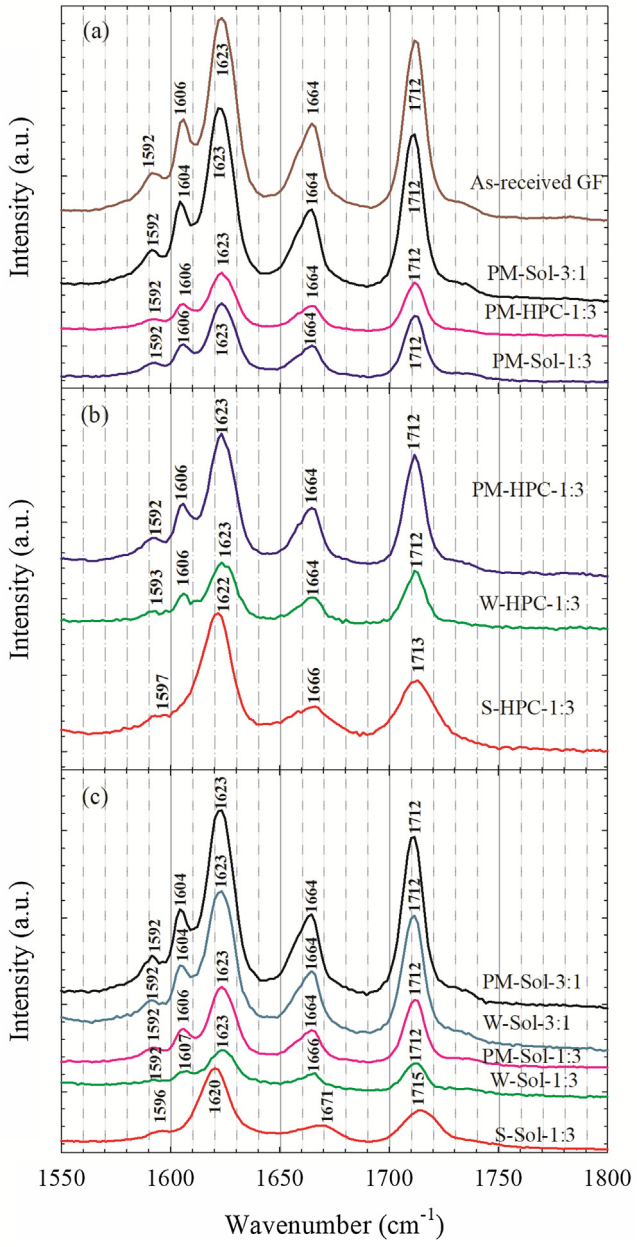

Fig. 7. Raman spectra of as-received GF, physical mixtures (PMs) of GF–Sol–SDS at 3:1 and 1:3 GF:Sol mass ratios and GF–HPC–SDS at 1:3 GF:HPC mass ratio (a); physical mixtures of GF–polymer–SDS and the spray-dried powders prepared using the GF nanosuspension-based (W) feed and GF solution-based (S) feed with 1:3 GF:polymer mass ratio: HPC as the polymer (b) and Sol as the polymer (c). W-Sol-3:1 stands for the spray-dried powder with 3:1 GF:Sol mass ratio.

desupersaturation experiments were performed. The GF desupersaturation curves indicate the superior GF recrystallization inhibition and supersaturation maintenance capability of Sol over HPC, and even at 1:1 drug:Sol mass ratio, Sol is an effective inhibitor (Fig. 9). Fig. 9 also corroborates the fast recrystallization tendency of GF [57] and suggests insignificant inhibition/promotion effect of SDS alone on recrystallization. Again, these findings from the desupersaturation experiments can be explained by adequate GF–Sol miscibility based on solubility parameter differences and stronger GF–Sol molecular interactions than GF–HPC interactions, based on Raman spectroscopy (Fig. 7).

3.5. Dissolution performance of the spray-dried powders

The temporal evolution of GF release from the spray-dried powders and their corresponding PMs containing 100 mg equivalent GF dose in 1000 mL deionized water was investigated. We note from Figs. 10 and 11 that the mere presence of HPC/Sol–SDS in PMs could slightly increase the extent and rate of GF release without any prior processing of the as-received GF particles, except blending. This could be partly explained by the wetting enhancement of the hydrophobic drug (GF) in the presence of HPC/Sol–SDS and deaggregation of the large drug aggregates present in the as-received drug [17] and partly by the higher solubility in the dissolution medium. The thermodynamic solubility of the GF microparticles at 37 °C was measured to be 14.2 mg/L, 17.8 mg/L, and 18.3 mg/L in the deionized water, aqueous medium of Sol–SDS (1:3 drug:polymer ratio), and aqueous medium of HPC–SDS (1:3 drug:polymer ratio), respectively.

Figs. 10 and 11 also show that both GF HyNASDs and ASDs prepared via spray-drying of the suspension-based (W) and solution-based (S) feeds, respectively, enhanced the dissolution rate and the extent of GF release as compared to the as-received GF and the physical mixtures (PMs). However, even a cursory look at the Fig. 10 vs. Fig. 11 reveals a drastic difference between HPC-based formulations and Sol-based formulations: the former provided an order of magnitude lower (relative) supersaturation than the latter, i.e., ~50% (for both HyNASDs and ASDs) vs. 360% (S-Sol-1:3, ASD) and 180% (W-Sol-1:3, HyNASD). Another interesting general observation is that there was little impact of polymer loading or drug:polymer ratio on the supersaturation for HPC-based formulations, whereas supersaturation significantly increased upon increase in polymer loading (lower drug:polymer ratio) for Sol-based formulations.

HPC-based HyNASDs and ASDs performed equally poorly in enhancing supersaturation (Fig. 10), but for different reasons, as compared with Sol-based HyNASDs and ASDs (Fig. 11). S-HPC-1:1 and S-HPC-1:3 powders are ASDs that have respectively 94% and 100% XRPD-amorphous GF, which has order of magnitude higher apparent (kinetic) solubility than its crystalline counterpart. Unfortunately, depending on the polymer–drug miscibility and interactions, amorphous drugs may phase-separate and recrystallize upon contact of ASDs with water in the dissolution medium [82,83] because once imbibed into the ASD matrix, water acts as a plasticizing agent, reducing the T_g of the ASD and enhancing the mobility of the drug molecules [83]. HPC-SSL has sub-ambient T_g [75] (lower than T_g of Sol: 73 ± 2 °C) and its ASDs have lower T_g than Sol-based ASDs (see Table 4). Moreover, due to HPC immiscibility with GF, its relatively weak molecular interactions with GF as compared with Sol (miscible with GF), as well as its poor GF nucleation/crystal growth inhibition (refer to Fig. 9), it is no surprise that the amorphous GF recrystallized from HPC-based ASDs during the dissolution test, which also explains the drastic differences between the HPC-based ASDs vs. Sol-based ASDs. PLM images of a loose compact of the ASD particles in Fig. 12 also corroborate the formation of GF crystals from S-HPC-1:3 ASD upon its exposure to water, whereas no recrystallization was observed for S-Sol-1:3. The HPC-based HyNASDs also performed poorly. Although they released GF nanocrystals upon redispersion (see Section S.1 of *Supplementary Material*), these GF nanocrystals have limited supersaturation capability. Moreover, the small amorphous content of the HyNASDs probably recrystallized in water similar to amorphous GF in HPC-based ASDs. While HPC has been used in both marketed drug nanocrystal products and in academia for preparation of drug nanosuspensions and drug nanocomposites [16,28], we find here that its SSL grade is not a suitable for preventing GF recrystallization and achieving high GF supersaturation.

What is remarkable about the dissolution results in Fig. 11 is neither the 360% supersaturation obtained with the S-Sol-1:3 ASD nor the higher Sol loading (1:3 vs. 1:1 GF:Sol ratio) achieving higher supersaturation. ASDs are well-known to generate significant supersaturation [82,84] due to amorphous nature of the molecularly dispersed drug,

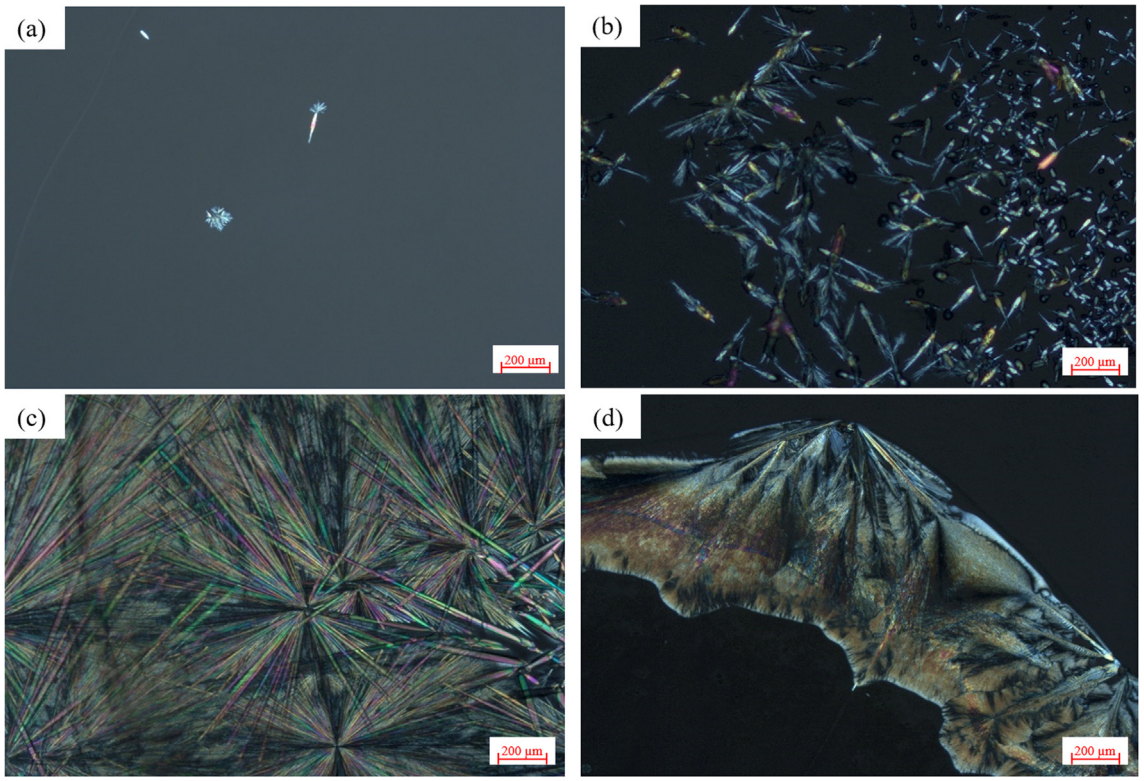

Fig. 8. Polarized light microscope images of a droplet of GF solution-based (S) feed, i.e., (a) S-Sol-1:3, (b) S-Sol-1:1, (c) S-HPC-1:3, and (d) S-HPC-1:1, dried on a hot glass slide at 75 °C. All images were taken at 5X zoom (scale bar: 200 μm).

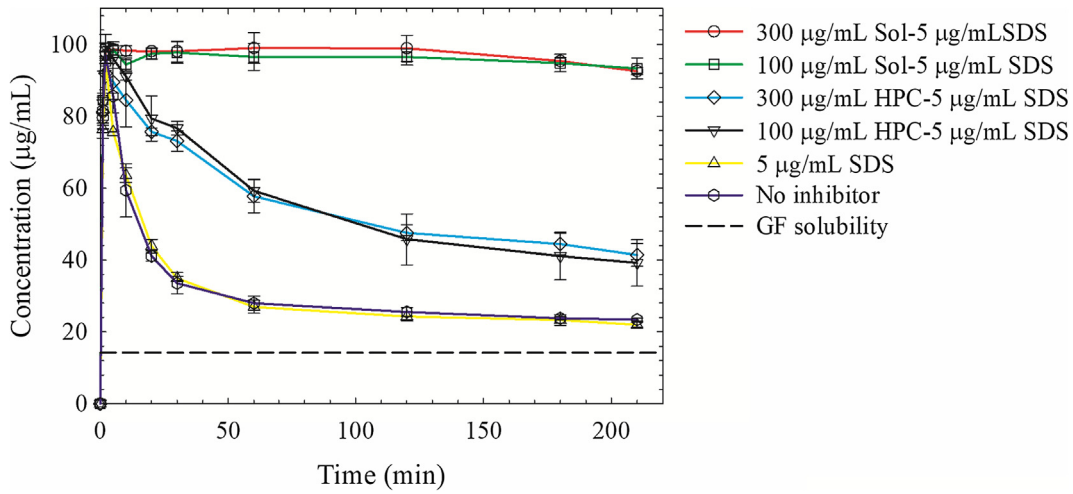

Fig. 9. GF desupersaturation curves for a supersaturated 20 mL GF–acetone solution mixed with 1000 mL aqueous solution of 300 μg/mL and 100 μg/mL of HPC/Sol–5 μg/mL SDS (equivalent to S-formulations with 1:3 and 1:1 drug:polymer mass ratios, respectively), 5 μg/mL SDS only, and in the absence of any recrystallization inhibitor. The initial GF concentration right after mixing ranged from 92 to 99 μg/mL.

and the polymer provides solubilization of the drug within the swollen GF–Sol matrix and recrystallization inhibition. Sol has a T_g of 73 ± 2 °C and strong molecular interactions with GF (GF Raman line shifts in Fig. 7); it is miscible with GF and is an excellent GF nucleation/crystal growth inhibitor, as evidenced by the small desupersaturation after ~3 h (Fig. 9) and absence of crystals in the PLM image (Fig. 12b). During the PLM imaging of S-Sol-1:3 (see Fig. 12b), the compact with the Sol matrix got swollen after the addition of water while eroding slowly (not shown in the images). Even after 5 min of water imbibition, no recrystallization of the amorphous GF was observed, which supports how high supersaturation was reached in this ASD.

What we found surprising is that W-Sol-1:3 provides 180% GF supersaturation (Fig. 11). It is well-known that drug nanocomposites have limited supersaturation capability, typically up to 10–15% [23], and supersaturation capability of nanocomposites has not even been studied in depth [26,27,39]. Note that W-Sol-1:3 is not a traditional nanocomposite: while largely composed of drug nanocrystals, it has about 20% amorphous GF and in water it provided 180% supersaturation. In this paper, we refer to such nanocomposites as HyNASDs (Fig. 6b) to differentiate them from nanocomposites (Fig. 6a) and ASDs (Fig. 6b). Another remarkable finding is that W-Sol-1:3 (HyNASD) generated more supersaturation than S-Sol-1:1 (ASD), i.e., 180% vs. 130%. Although this mainly resulted from the HyNASD having more Sol than the ASD and this comparison is not head-to-head, there is no

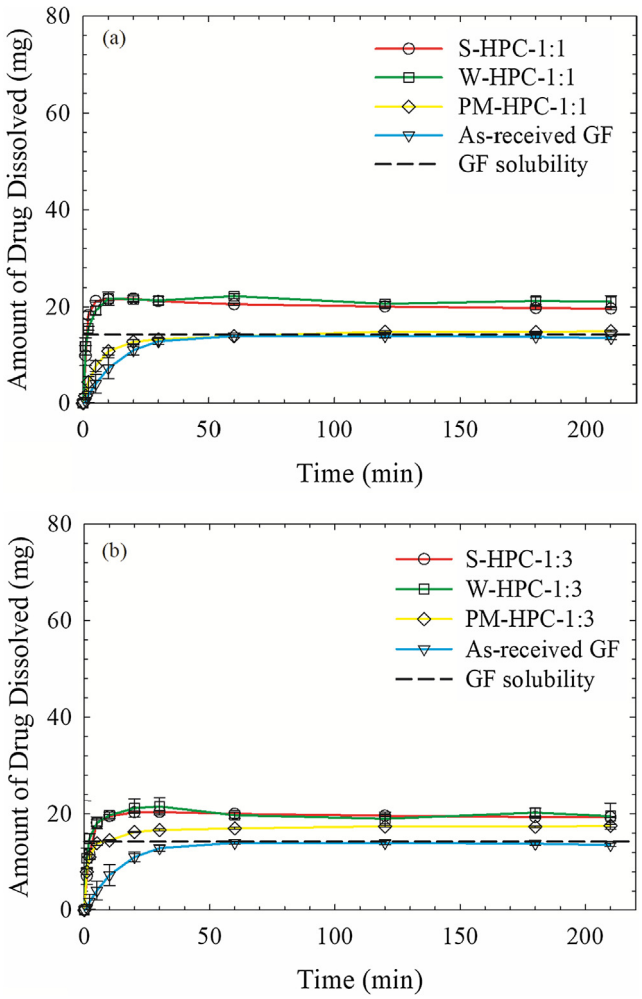

Fig. 10. Evolution of drug release from as-received GF, physical mixture (PM) of GF–HPC–SDS, and spray-dried powders with two different GF:HPC mass ratios: (a) 1:1 GF:HPC and (b) 1:3 GF:HPC. Dissolution sample size is equivalent to 100 mg GF dose.

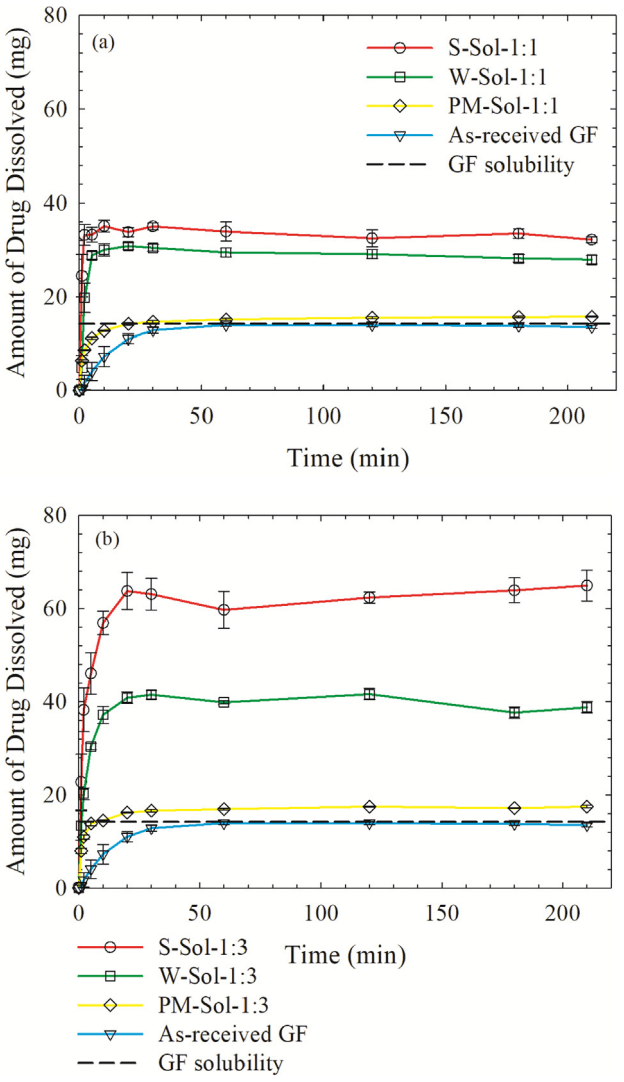

Fig. 11. Evolution of drug release from as-received GF, physical mixture (PM) of GF–Sol–SDS, and spray-dried powders with two different GF:Sol mass ratios: (a) 1:1 GF:Sol and (b) 1:3 GF:Sol. Dissolution sample size is equivalent to 100 mg GF dose.

similar result in literature where a formulation consisting of ~80% nanocrystals outperforms an ASD with 100% amorphous drug. Clearly, HyNASDs boost the supersaturating capabilities of traditional nanocomposites.

3.6. Dissolution performance of HyNASDs vs. Traditional nanocomposites and GF size effect

Additional dissolution experiments were carried out with various spray-dried powders prepared using suspension-based (W) feeds in order to elucidate the significant functional performance difference between traditional nanocomposites (e.g. W-Sol-3:1 with low Sol loading) and HyNASDs (W-Sol-1:1 and W-Sol-1:3 with high Sol loading) (see Fig. 13). Note that the precursor GF nanosuspensions used in the spray drying for these formulations had about the same GF nanoparticle size, i.e., d_{50} = 0.14–0.16 μm. W-Sol-3:1, like any traditional nanocomposite, provided low (30%) supersaturation, whereas the two HyNASDs, i.e., W-Sol-1:1 and W-Sol-1:3, provided 100% and 180% supersaturation, respectively. There is a clear trend: an increase in Sol loading led to higher amorphous content and higher GF supersaturation/drug release, while the precursors GF nanoparticle suspensions used to prepare these spray-dried powders did not have drastically different GF particle sizes.

During dissolution of the HyNASDs, the amorphous GF dissolves and diffuses through swollen Sol matrix [17], while additional GF could dissolve into the swollen Sol matrix and supersaturate upon water imbibition. It is also likely that higher Sol loading helps the solubilization in the dissolution medium. Not only did the higher Sol content lead to HyNASDs having higher amorphous content upon spray drying (see Table 4), but also the higher Sol loading enabled solubilization of additional GF within the swollen Sol matrix and/or in the dissolution medium. Both mechanisms contributed to the high supersaturation from HyNASDs. The contribution of amorphous GF and GF solubilization by Sol to supersaturation follows the order: W-Sol-1:3 (180%) > W-Sol-1:1 (eq. 1:3) (130%) > W-Sol-1:1 (100%) (Fig. 13). Note that W-Sol-1:1 (eq. 1:3) has the same total Sol content as in W-Sol-1:3, but 2/3rd of Sol was pre-dissolved in the dissolution medium and it was not part of the W-Sol-1:1 matrix. Incorporating the whole Sol in the spray-dried matrix achieved higher supersaturation than keeping 1/3rd of Sol in the matrix and pre-dissolving 2/3rd in the medium. Apparently, having all Sol in the spray-dried matrix allowed for more amorphous GF generated during the spray-drying, while also helping the solubilization of GF within the swollen Sol matrix. On the other hand, having additional Sol in the dissolution medium generated more supersaturation, as inferred from the dissolution of W-Sol-1:1 (eq. 1:3) vs. W-Sol-1:1.

It may be argued that the higher supersaturation in HyNASDs as

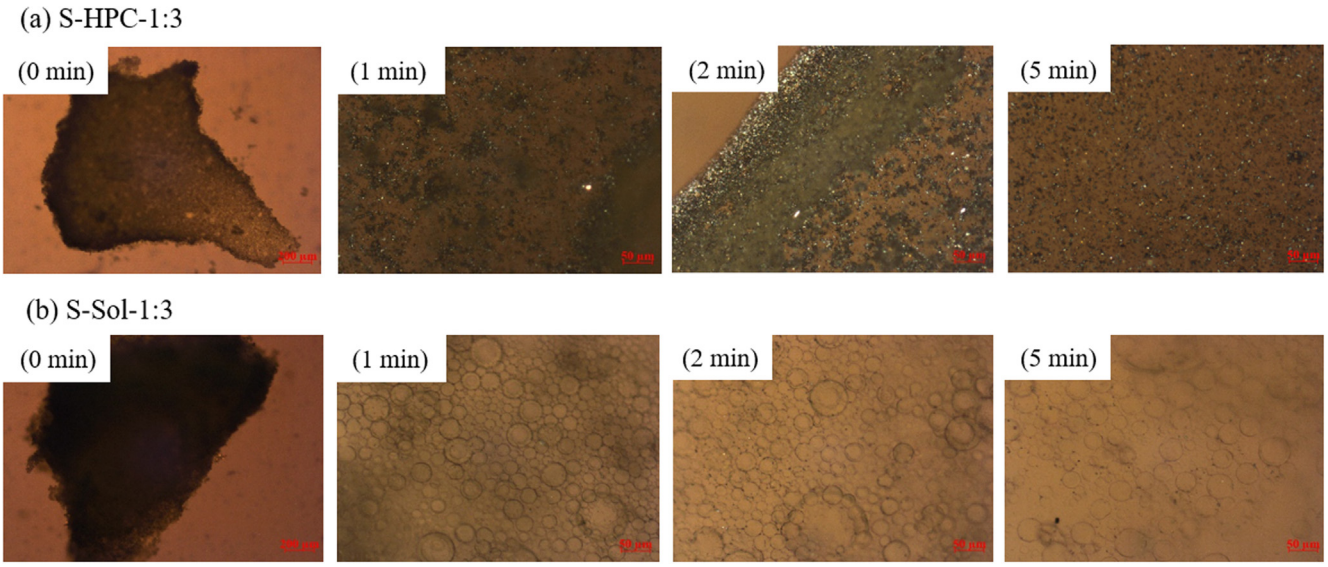

Fig. 12. Polarized light microscope images of a loose compact of the ASD particles (S-formulations) with (a) 1:3 GF:HPC mass ratio and (b) 1:3 GF:Sol mass ratio in 20 μL deionized water. The images were taken at 0 (before adding water), 1, 2, and 5 min after the addition of deionized water addition. Except 0 min image (5X magnification, scale bar: 200 μm), which focused on the compact, all other images focused on particles that emanated from the surface, which were captured at 20X magnification (scale bar: 50 μm).

compared with traditional nanocomposites is solely about GF–Sol interactions/miscibility and GF solubilization by Sol. W-M-Sol-1:3 was prepared by spray-drying the aqueous suspension of as-received (micronized, d_{50}: 10.0 μm) GF microcrystals with Sol–SDS. W-Sol-1:3 (HyNASD), which contains drug nanocrystals with d_{50}: 0.14 μm and ~20% amorphous GF, generated thrice as much supersaturation as W-M-Sol-1:3, demonstrating the importance of particle size in HyNASD for supersaturation generation. The solubilization of GF particles (microparticles or nanoparticles) in the Sol matrix and supersaturation generation during the dissolution is a kinetically-driven process, which is limited by the size of the particles: faster solubilization and higher supersaturation occurred when GF nanoparticles were encapsulated by the Sol matrix (HyNASD) as compared with the micronized GF particles owing to approximately 70-times larger surface area of the nanoparticles.

4. Conclusions

Spray-drying of an aqueous GF nanosuspension with 1:1 and 1:3 GF:Sol/HPC mass ratios in the presence of SDS led to formation HyNASDs, which have notable amorphous GF content unlike traditional drug nanocomposites that typically have 1:0.8 to 1:0.02 drug:polymer mass ratio. To ensure a fair, head-to-head comparison of HyNASDs to ASDs, ASDs with identical composition were prepared by spray-drying the organic solution of GF–Sol/HPC–SDS in acetone–water mixture. All spray-dried powders had acceptable content uniformity. XRPD–DSC–Raman spectroscopy shed light on the nanocomposite/HyNASD and ASD formation. HPC-based HyNASDs and ASDs performed equally poorly in enhancing GF supersaturation (50%) in dissolution tests, whereas Sol-based ones achieved significant supersaturation: up to 360% for ASD and 180% for HyNASD. These results were explained by higher T_g of Sol than that of HPC, GF–Sol miscibility, stronger molecular interactions between Sol–GF than HPC–GF, and excellent nucleation/crystal growth inhibition by Sol as compared to

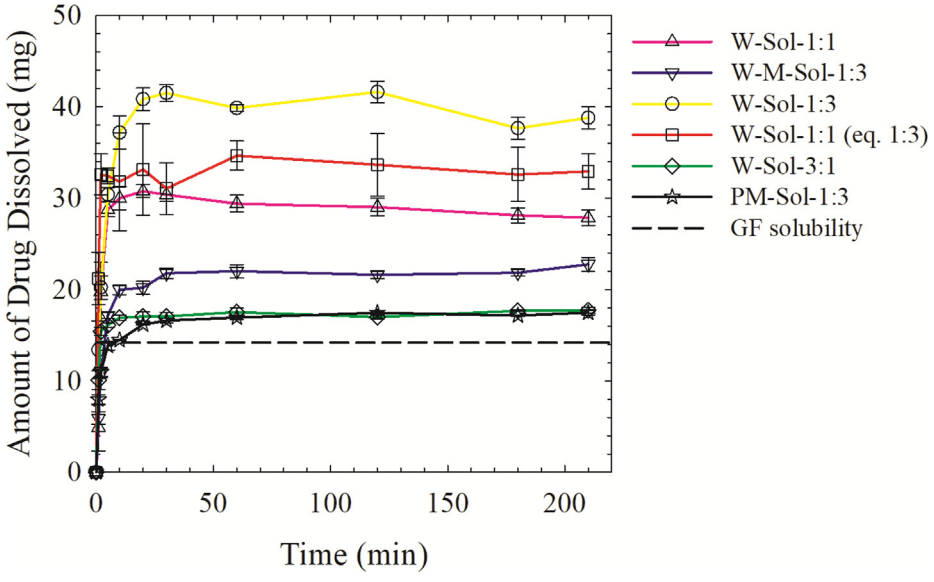

Fig. 13. Evolution of GF dissolution from physical mixture (PM) of GF–Sol–SDS with 1:3 GF:Sol, spray-dried W-formulations with 1:1, 1:3, and 3:1 GF:Sol, as well as W-Sol-1:1 (eq. 1:3), which has the same total Sol content as in W-Sol-1:3, but 2/3rd of Sol was pre-dissolved in the dissolution medium and the remaining 1/3rd was in W-Sol-1:1 (eq. 1:3). W-M-Sol-1:3 stands for the spray-dried powder prepared using a suspension-based feed of as-received (micronized) GF. Dissolution sample size is equivalent to 100 mg GF dose.

HPC. The supersaturation generation capability of HyNASDs is largely controlled by drug–polymer interactions/miscibility as well as the size of the drug (nano)crystals in the polymeric matrix. Overall, the most striking finding from this study is that despite having ~80% nanocrystals, HyNASDs provided fast drug supersaturation (~190% within 20 min) unlike traditional nanocomposites (30%), which could render nanoparticle formulations more attractive in bioavailability enhancement of poorly soluble drugs. While HyNASDs did not generate as high saturation as ASDs, they can be rendered competitive to ASDs upon further formulation–process optimization. Future research efforts will include (i) investigation of the storage stability of HyNASDs vs. ASDs under various environmental conditions, (ii) preparation of HyNASDs with various drug–polymer pairs and their comparative assessment, (iii) systematic examination of the impact of various surfactants, and (iv) impact of various drug nanoparticle sizes in the range of 50–1000 nm on drug supersaturation.

Appendix A. Supplementary material

Supplementary data to this article can be found online at https://doi.org/10.1016/j.ejpb.2019.10.002.

References

[1] L.Z. Benet, C.Y. Wu, J.M. Custodio, Predicting drug absorption and the effects of food on oral bioavailability, Bull. Tech. Gattefosse 99 (2006) 9–16.
[2] C.W. Pouton, Formulation of poorly water-soluble drugs for oral administration: physicochemical and physiological issues and the lipid formulation classification system, Eur. J. Pharm. Sci. 29 (2006) 278–287.
[3] A. Müllertz, A. Ogbonna, S. Ren, T. Rades, New perspectives on lipid and surfactant based drug delivery systems for oral delivery of poorly soluble drugs, J. Pharm. Pharmacol. 62 (2010) 1622–1636.
[4] A.C. Rumondor, S.S. Dhareshwar, F. Kesisoglou, Amorphous solid dispersions or prodrugs: complementary strategies to increase drug absorption, J. Pharm. Sci. 105 (2016) 2498–2508.
[5] K. Letchford, H. Burt, A review of the formation and classification of amphiphilic block copolymer nanoparticulate structures: micelles, nanospheres, nanocapsules and polymersomes, Eur. J. Pharm. Biopharm. 65 (2007) 259–269.
[6] N. Schultheiss, A. Newman, Pharmaceutical cocrystals and their physicochemical properties, Cryst. Growth Des. 9 (2009) 2950–2967.
[7] D. Singhal, W. Curatolo, Drug polymorphism and dosage form design: a practical perspective, Adv. Drug Delivery Rev. 56 (2004) 335–347.
[8] Z. Rahman, A.S. Zidan, R. Samy, V.A. Sayeed, M.A. Khan, Improvement of physicochemical properties of an antiepileptic drug by salt engineering, AAPS PharmSciTech 13 (2012) 793–801.
[9] O. Aleem, B. Kuchekar, Y. Pore, S. Late, Effect of β-cyclodextrin and hydroxypropyl β-cyclodextrin complexation on physicochemical properties and antimicrobial activity of cefdinir, J. Pharm. Biomed. Anal. 47 (2008) 535–540.
[10] A.J. Humberstone, W.N. Charman, Lipid-based vehicles for the oral delivery of poorly water soluble drugs, Adv. Drug Delivery Rev. 25 (1997) 103–128.
[11] E. Merisko-Liversidge, G.G. Liversidge, E.R. Cooper, Nanosizing: a formulation approach for poorly-water-soluble compounds, Eur. J. Pharm. Sci. 18 (2003) 113–120.
[12] A. Serajuddin, Solid dispersion of poorly water-soluble drugs: Early promises, subsequent problems, and recent breakthroughs, J. Pharm. Sci. 88 (1999) 1058–1066.
[13] F. Kesisoglou, S. Panmai, Y. Wu, Nanosizing—oral formulation development and biopharmaceutical evaluation, Adv. Drug Delivery Rev. 59 (2007) 631–644.
[14] R.H. Müller, S. Gohla, C.M. Keck, State of the art of nanocrystals–special features, production, nanotoxicology aspects and intracellular delivery, Eur. J. Pharm. Biopharm. 78 (2011) 1–9.
[15] C. Brough, R. Williams, Amorphous solid dispersions and nano-crystal technologies for poorly water-soluble drug delivery, Int. J. Pharm. 453 (2013) 157–166.
[16] A. Bhakay, M. Rahman, R.N. Dave, E. Bilgili, Bioavailability enhancement of poorly water-soluble drugs via nanocomposites: Formulation processing aspects and challenges, Pharmaceutics 10 (2018).
[17] M. Li, N. Ioannidis, C. Gogos, E. Bilgili, A comparative assessment of nanocomposites vs. amorphous solid dispersions prepared via nanoextrusion for drug dissolution enhancement, Eur. J. Pharm. Biopharm. 119 (2017) 68–80.
[18] S.K. Singh, K. Srinivasan, K. Gowthamarajan, D.S. Singare, D. Prakash, N.B. Gaikwad, Investigation of preparation parameters of nanosuspension by top-down media milling to improve the dissolution of poorly water-soluble glyburide, Eur. J. Pharm. Biopharm. 78 (2011) 441–446.
[19] Y. Tanaka, M. Inkyo, R. Yumoto, J. Nagai, M. Takano, S. Nagata, Nanoparticulation of probucol, a poorly water-soluble drug, using a novel wet-milling process to improve in vitro dissolution and in vivo oral absorption, Drug Dev. Ind. Pharm. 38 (2012) 1015–1023.
[20] A. Tuomela, P. Liu, J. Puranen, S. Rönkkö, T. Laaksonen, G. Kalesnykas, O. Oksala, J. Ilkka, J. Laru, K. Järvinen, Brinzolamide nanocrystal formulations for ophthalmic delivery: reduction of elevated intraocular pressure in vivo, Int. J. Pharm. 467 (2014) 34–41.
[21] A.A. Noyes, W.R. Whitney, The rate of solution of solid substances in their own solutions, J. Am. Chem. Soc. 19 (1897) 930–934.
[22] R.H. Müller, S. Benita, B.H. Böhm, Nanosuspensions, in: S. Benita, B.H. Böhm (Eds.), Emulsions and nanosuspensions for the formulation of poorly soluble drugs, Medpharm Scientific, Stuttgart, Germany, 1998, pp. 149–173.
[23] F. Kesisoglou, Y. Wu, Understanding the effect of API properties on bioavailability through absorption modeling, AAPS J. 10 (2008) 516–525.
[24] R.H. Müller, K. Peters, Nanosuspensions for the formulation of poorly soluble drugs: I. Preparation by a size-reduction technique, Int. J. Pharm. 160 (1998) 229–237.
[25] Q. Fu, J. Sun, D. Zhang, M. Li, Y. Wang, G. Ling, X. Liu, Y. Sun, X. Sui, C. Luo, Nimodipine nanocrystals for oral bioavailability improvement: preparation, characterization and pharmacokinetic studies, Coll. Surf. B Biointerf. 109 (2013) 161–166.
[26] A. Bhakay, M. Azad, E. Bilgili, R. Dave, Redispersible fast dissolving nanocomposite microparticles of poorly water-soluble drugs, Int. J. Pharm. 461 (2014) 367–379.
[27] M. Azad, C. Arteaga, B. Abdelmalek, R. Davé, E. Bilgili, Spray drying of drug-swellable dispersant suspensions for preparation of fast-dissolving, high drug-loaded, surfactant-free nanocomposites, Drug Dev. Ind. Pharm. 41 (2015) 1617–1631.
[28] M. Li, M. Azad, R. Davé, E. Bilgili, Nanomilling of drugs for bioavailability enhancement: a holistic formulation–process perspective, Pharmaceutics 8 (2016) 27.
[29] Y. Wang, Y. Zheng, L. Zhang, Q. Wang, D. Zhang, Stability of nanosuspensions in drug delivery, J. Controlled Release 172 (2013) 1126–1141.
[30] C. Knieke, M. Azad, R. Davé, E. Bilgili, A study of the physical stability of wet media-milled fenofibrate suspensions using dynamic equilibrium curves, Chem. Eng. Res. Des. 91 (2013) 1245–1258.
[31] M. Li, N. Lopez, E. Bilgili, A study of the impact of polymer–surfactant in drug nanoparticle coated pharmatose composites on dissolution performance, Adv. Powder Technol. 27 (2016) 1625–1636.
[32] I. Ghosh, S. Bose, R. Vippagunta, F. Harmon, Nanosuspension for improving the bioavailability of a poorly soluble drug and screening of stabilizing agents to inhibit crystal growth, Int. J. Pharm. 409 (2011) 260–268.
[33] S. Verma, S. Kumar, R. Gokhale, D.J. Burgess, Physical stability of nanosuspensions: investigation of the role of stabilizers on Ostwald ripening, Int. J. Pharm. 406 (2011) 145–152.
[34] T.-L. Chang, H. Zhan, D. Liang, J.F. Liang, Nanocrystal technology for drug formulation and delivery, Front. Chem. Sci. Eng. 9 (2015) 1–14.
[35] B. Van Eerdenbrugh, G. Van den Mooter, P. Augustijns, Top-down production of drug nanocrystals: nanosuspension stabilization, miniaturization and transformation into solid products, Int. J. Pharm. 364 (2008) 64–75.
[36] S. Kumar, X. Xu, R. Gokhale, D.J. Burgess, Formulation parameters of crystalline nanosuspensions on spray drying processing: a DoE approach, Int. J. Pharm. 464 (2014) 34–45.
[37] X. Zhang, J. Guan, R. Ni, L.C. Li, S. Mao, Preparation and solidification of redispersible nanosuspensions, J. Pharm. Sci. 103 (2014) 2166–2176.
[38] S. Kumar, J. Shen, B. Zolnik, N. Sadrieh, D.J. Burgess, Optimization and dissolution performance of spray-dried naproxen nano-crystals, Int. J. Pharm. 486 (2015) 159–166.
[39] D.A. Shah, M. Patel, S.B. Murdande, R.H. Dave, Influence of spray drying and dispersing agent on surface and dissolution properties of griseofulvin micro and nanocrystals, Drug Dev. Ind. Pharm. 42 (2016) 1842–1850.
[40] Y. Hou, J. Shao, Q. Fu, J. Li, J. Sun, Z. He, Spray-dried nanocrystals for a highly hydrophobic drug: Increased drug loading, enhanced redispersity, and improved oral bioavailability, Int. J. Pharm. 516 (2017) 372–379.
[41] C. Konnerth, V. Braig, A. Ito, J. Schmidt, G. Lee, W. Peukert, Formation of mefenamic acid nanocrystals with improved dissolution characteristics, Chem. Ing. Tech. 89 (2017) 1060–1071.
[42] F. Toziopoulou, M. Malamatari, I. Nikolakakis, K. Kachrimanis, Production of aprepitant nanocrystals by wet media milling and subsequent solidification, Int. J. Pharm. 533 (2017) 324–334.
[43] D. Medarević, J. Djuriš, S. Ibrić, M. Mitrić, K. Kachrimanis, Optimization of formulation and process parameters for the production of carvedilol nanosuspension by wet media milling, Int. J. Pharm. 540 (2018) 150–161.
[44] S. Aleandri, M. Schönenberger, A. Niederquell, M. Kuentz, Temperature-induced surface effects on drug nanosuspensions, Pharm. Res. 35 (2018) 69.
[45] M. Li, I. Suriel, J. Vekaria, J. Proske, P. Orbe, M. Armani, R. Dave, E. Bilgili, Impact of dispersants on dissolution of itraconazole from drug-loaded, surfactant-free, spray-dried nanocomposites, Powder Technol. 339 (2018) 281–295.
[46] E. Bilgili, M. Rahman, D. Palacios, F. Arevalo, Impact of polymers on the aggregation of wet-milled itraconazole particles and their dissolution from spray-dried nanocomposites, Adv. Powder Technol. 9 (2018) 2941–2956.
[47] S. Basa, T. Muniyappan, P. Karatgi, R. Prabhu, R. Pillai, Production and in vitro characterization of solid dosage form incorporating drug nanoparticles, Drug Dev. Ind. Pharm. 34 (2008) 1209–1218.
[48] B. Van Eerdenbrugh, L. Froyen, J. Van Humbeeck, J.A. Martens, P. Augustijns, G. Van den Mooter, Drying of crystalline drug nanosuspensions—the importance of surface hydrophobicity on dissolution behavior upon redispersion, Eur. J. Pharm. Sci. 35 (2008) 127–135.
[49] J. Lee, Drug nano-and microparticles processed into solid dosage forms: physical properties, J. Pharm. Sci. 92 (2003) 2057–2068.
[50] S. Poozesh, E. Bilgili, Scale-up of pharmaceutical spray drying using scale-up rules: a review, Int. J. Pharm. 562 (2019) 271–292.
[51] K. Yamashita, T. Nakate, K. Okimoto, A. Ohike, Y. Tokunaga, R. Ibuki, K. Higaki,

T. Kimura, Establishment of new preparation method for solid dispersion formulation of tacrolimus, Int. J. Pharm. 267 (2003) 79–91.
[52] K. Six, G. Verreck, J. Peeters, M. Brewster, G. Van den Mooter, Increased physical stability and improved dissolution properties of itraconazole, a class II drug, by solid dispersions that combine fast-and slow-dissolving polymers, J. Pharm. Sci. 93 (2004) 124–131.
[53] A.A. Ambike, K. Mahadik, A. Paradkar, Spray-dried amorphous solid dispersions of simvastatin, a low Tg drug: in vitro and in vivo evaluations, Pharm. Res. 22 (2005) 990–998.
[54] P. Srinarong, H. de Waard, H.W. Frijlink, W.L. Hinrichs, Improved dissolution behavior of lipophilic drugs by solid dispersions: the production process as starting point for formulation considerations, Expert Opin. Drug Delivery 8 (2011) 1121–1140.
[55] S. Baghel, H. Cathcart, N.J. O'Reilly, Polymeric amorphous solid dispersions: a review of amorphization, crystallization, stabilization, solid-state characterization, and aqueous solubilization of biopharmaceutical classification system class II drugs, J. Pharm. Sci. 105 (2016) 2527–2544.
[56] M.G. Fakes, B.J. Vakkalagadda, F. Qian, S. Desikan, R.B. Gandhi, C. Lai, A. Hsieh, M.K. Franchini, H. Toale, J. Brown, Enhancement of oral bioavailability of an HIV-attachment inhibitor by nanosizing and amorphous formulation approaches, Int. J. Pharm. 370 (2009) 167–174.
[57] J.A. Baird, B. Van Eerdenbrugh, L.S. Taylor, A classification system to assess the crystallization tendency of organic molecules from undercooled melts, J. Pharm. Sci. 99 (2010) 3787–3806.
[58] M. Kataoka, Y. Masaoka, Y. Yamazaki, T. Sakane, H. Sezaki, S. Yamashita, In vitro system to evaluate oral absorption of poorly water-soluble drugs: simultaneous analysis on dissolution and permeation of drugs, Pharm. Res. 20 (2003) 1674–1680.
[59] FDA Database, GRIS-PEG (GRISEOFULVIN ULTRAMICROSIZE) TABLETS, USP 125 MG; 250 MG, 2016 (7 Oct 2019), Reference ID: 3919275. https://www.accessdata.fda.gov/drugsatfda_docs/label/2016/050475s057lbl.pdf.
[60] D. Zhou, G.G. Zhang, D. Law, D.J. Grant, E.A. Schmitt, Thermodynamics, molecular mobility and crystallization kinetics of amorphous griseofulvin, Mol. Pharmaceut. 5 (2008) 927–936.
[61] G. Terife, P. Wang, N. Faridi, C.G. Gogos, Hot melt mixing and foaming of soluplus® and indomethacin, Polym. Eng. Sci. 52 (2012) 1629–1639.
[62] E.-S. Ha, I.-H. Baek, W. Cho, S.-J. Hwang, M.-S. Kim, Preparation and evaluation of solid dispersion of atorvastatin calcium with Soluplus® by spray drying technique, Chem. Pharm. Bull. 62 (2014) 545–551.
[63] A. Afolabi, O. Akinlabi, E. Bilgili, Impact of process parameters on the breakage kinetics of poorly water-soluble drugs during wet stirred media milling: a microhydrodynamic view, Eur. J. Pharm. Sci. 51 (2014) 75–86.
[64] E. Bilgili, M. Li, A. Afolabi, Is the combination of cellulosic polymers and anionic surfactants a good strategy for ensuring physical stability of BCS Class II drug nanosuspensions? Pharm. Dev. Technol. 21 (2016) 499–510.
[65] H. Konno, T. Handa, D.E. Alonzo, L.S. Taylor, Effect of polymer type on the dissolution profile of amorphous solid dispersions containing felodipine, Eur. J. Pharm. Biopharm. 70 (2008) 493–499.
[66] E. Bilgili, A. Afolabi, A combined microhydrodynamics–polymer adsorption analysis for elucidation of the roles of stabilizers in wet stirred media milling, Int. J. Pharm. 439 (2012) 193–206.
[67] H. Yang, F. Teng, P. Wang, B. Tian, X. Lin, X. Hu, L. Zhang, K. Zhang, Y. Zhang, X. Tang, Investigation of a nanosuspension stabilized by Soluplus® to improve bioavailability, Int. J. Pharm. 477 (2014) 88–95.
[68] A. Monteiro, A. Afolabi, E. Bilgili, Continuous production of drug nanoparticle suspensions via wet stirred media milling: a fresh look at the Rehbinder effect, Drug Dev. Ind. Pharm. 39 (2013) 266–283.
[69] P. Kayaert, G. Van den Mooter, Is the amorphous fraction of a dried nanosuspension caused by milling or by drying? A case study with Naproxen and Cinnarizine, Eur. J. Pharm. Biopharm. 81 (2012) 650–656.
[70] D.J. Greenhalgh, A.C. Williams, P. Timmins, P. York, Solubility parameters as predictors of miscibility in solid dispersions, J. Pharm. Sci. 88 (1999) 1182–1190.
[71] A. Forster, J. Hempenstall, T. Rades, Characterization of glass solutions of poorly water-soluble drugs produced by melt extrusion with hydrophilic amorphous polymers, J. Pharm. Pharmacol. 53 (2001) 303–315.
[72] S. Thakral, N.K. Thakral, Prediction of drug–polymer miscibility through the use of solubility parameter based Flory-Huggins interaction parameter and the experimental validation: PEG as model polymer, J. Pharm. Sci. 102 (2013) 2254–2263.
[73] P. Choi, T.A. Kavassalis, A. Rudin, Estimation of Hansen solubility parameters for (hydroxyethyl) and (hydroxypropyl) cellulose through molecular simulation, Ind. Eng. Chem. Res. 33 (1994) 3154–3159.
[74] K. Kolter, M. Karl, A. Gryczke, B. Ludwigshafen am Rhein, Hot-melt extrusion with BASF pharma polymers: extrusion compendium, BASF, 2012.
[75] A. Sarode, P. Wang, C. Cote, D.R. Worthen, Low-viscosity hydroxypropylcellulose (HPC) grades SL and SSL: versatile pharmaceutical polymers for dissolution enhancement, controlled release, and pharmaceutical processing, AAPS PharmSciTech 14 (2013) 151–159.
[76] K. Wlodarski, W. Sawicki, A. Kozyra, L. Tajber, Physical stability of solid dispersions with respect to thermodynamic solubility of tadalafil in PVP-VA, Eur. J. Pharm. Biopharm. 96 (2015) 237–246.
[77] C. Luebbert, F. Huxoll, G. Sadowski, Amorphous-amorphous phase separation in API/polymer formulations, Mol. 22 (2017) 296.
[78] T. Feng, R. Pinal, M.T. Carvajal, Process induced disorder in crystalline materials: differentiating defective crystals from the amorphous form of griseofulvin, J. Pharm. Sci. 97 (2008) 3207–3221.
[79] A. Żarów, B. Zhou, X. Wang, R. Pinal, Z. Iqbal, Spectroscopic and X-ray diffraction study of structural disorder in cryomilled and amorphous griseofulvin, Appl. Spectrosc. 65 (2011) 135–143.
[80] P. Mistry, S. Mohapatra, T. Gopinath, F.G. Vogt, R. Suryanarayanan, Role of the strength of drug–polymer interactions on the molecular mobility and crystallization inhibition in ketoconazole solid dispersions, Mol. Pharmaceut. 12 (2015) 3339–3350.
[81] K. Kothari, V. Ragoonanan, R. Suryanarayanan, The role of polymer concentration on the molecular mobility and physical stability of nifedipine solid dispersions, Mol. Pharmaceut. 12 (2015) 1477–1484.
[82] D.E. Alonzo, Y. Gao, D. Zhou, H. Mo, G.G. Zhang, L.S. Taylor, Dissolution and precipitation behavior of amorphous solid dispersions, J. Pharm. Sci. 100 (2011) 3316–3331.
[83] Y. Chen, C. Liu, Z. Chen, C. Su, M. Hageman, M. Hussain, R. Haskell, K. Stefanski, F. Qian, Drug–polymer–water interaction and its implication for the dissolution performance of amorphous solid dispersions, Mol. Pharmaceut. 12 (2015) 576–589.
[84] M.J. Jackson, U.S. Kestur, M.A. Hussain, L.S. Taylor, Dissolution of danazol amorphous solid dispersions: supersaturation and phase behavior as a function of drug loading and polymer type, Mol. Pharmaceut. 13 (2015) 223–231.